Title

Resident microbes shape the vaginal epithelial glycan landscape

Journal

Science Translational Medicine, 15(724)

ISSN

1946-6234

Authors

Agarwal, Kavita

Choudhury, Biswa

Robinson, Lloyd S

et al.

Publication Date

2023-11-29

DOI

10.1126/scitranslmed.abp9599

Peer reviewed

HHS Public Access

Author manuscript

Sci Transl Med. Author manuscript; available in PMC 2024 November 29.

Published in final edited form as:

Sci Transl Med. 2023 November 29; 15(724): eabp9599. doi:10.1126/scitranslmed.abp9599.

Resident microbes shape the vaginal epithelial glycan landscape

Kavita Agarwal[1,2,3,4,10], **Biswa Choudhury**[4], **Lloyd S. Robinson**[1,2,11], **Sydney R. Morrill**[1,2,3,4], **Yasmine Bouchibiti**[5,6], **Daisy Chilin-Fuentes**[7], **Sara B. Rosenthal**[7], **Kathleen M. Fisch**[3,7], **Jeffrey F. Peipert**[8], **Carlito B. Lebrilla**[5,6], **Jenifer E. Allsworth**[9], **Amanda L. Lewis**[1,2,3,4,*], **Warren G. Lewis**[1,2,3,4,*]

[1]Department of Molecular Microbiology, Washington University School of Medicine, St. Louis, MO 63110, United States of America.

[2]Center for Women's Infectious Disease Research, Washington University School of Medicine, St. Louis, MO 63110, United States of America.

[3]Department of Obstetrics, Gynecology, and Reproductive Sciences, University of California San Diego (UCSD), La Jolla, CA 92093, United States of America.

[4]Glycobiology Research and Training Center, UCSD, La Jolla, CA 92093, United States of America.

[5]Department of Chemistry, University of California, Davis, Davis, CA 95616, United States of America.

[6]Department of Food Science and Technology, University of California, Davis, Davis, CA 95616, United States of America.

[7]Center for Computational Biology & Bioinformatics, UCSD, La Jolla, CA 92093, United States of America.

[8]Department of Obstetrics and Gynecology, Indiana University School of Medicine, Indianapolis, IN 46202, United States of America.

[9]Department of Biomedical and Health Informatics, University of Missouri, Kansas City School of Medicine, Kansas City, MO 64110, United States of America.

Abstract

[*]**Co-corresponding authors:** wglewis@health.ucsd.edu, a1lewis@health.ucsd.edu.

[10]Trivedi School of Biosciences, Ashoka University, Sonipat, Haryana 131029, India

[11]Omniose LLC, St. Louis, MO 63110, United States of America.

Author contributions

A.L.L., and W.G.L. conceived and supervised the project. K.A., B.C., A.L.L., and W.G.L. designed the experiments; K.A. performed enzyme assays, lectin analysis, imaging, flow cytometry, HPLC data acquisition, and RNA-seq experiments; B.C. acquired mass spectrometric and HPAEC data; Y.B. acquired LC-MS data for UC Bank specimens; L.S.R. expressed and purified NanH2 and NanH3 proteins; S.R.M. purified NanH2 from Clear Coli cells; K.A., L.S.R., S.R.M., and W.G.L performed blinded scoring of electron micrographs; D.C.F., S.B.R., and K.M.F. processed RNA-seq data; J. F. P. lead the inaugural Contraceptive CHOICE project from which specimens were originally archived, J.E.A. provided Nugent scoring data and performed analysis of demographic/clinical characteristics; K.A., B.C., Y.B., C.B.L., A.L.L., and W.G.L. performed data analysis; K.A., A.L.L., and W.G.L. made figures, and wrote the manuscript with input/approval from all the others.

Competing interests

Dr. Amanda Lewis is on the scientific advisory board of GlycoNet. Dr. Carlito B. Lebrilla is a co-founder and consultant for Infinant Health, InterVenn Bio, and BCD Bioscience. He is also a consultant for Turtle Tree. All other authors declare that they have no competing interests.

Epithelial cells are covered in carbohydrates (glycans). This glycan coat or “glycocalyx” interfaces directly with microbes, providing a protective barrier against potential pathogens. Bacterial vaginosis (BV) is a condition associated with adverse health outcomes in which bacteria reside in direct proximity to the vaginal epithelium. Some of these bacteria, including *Gardnerella*, produce glycosyl hydrolase enzymes. However, glycans of the human vaginal epithelial surface have not been studied in detail. Here we elucidate key characteristics of the ’normal’ vaginal epithelial glycan landscape and analyze the impact of resident microbes on the surface glycocalyx. In BV, the staining of the glycocalyx was visibly diminished in electron micrographs compared to controls. Biochemical and mass spectrometric analysis showed that, compared to ’normal’ vaginal epithelial cells, BV cells were depleted of sialylated *N*- and *O*-glycans, with underlying galactose residues exposed on the surface. Treatment of primary epithelial cells from BV-negative women with recombinant *Gardnerella* sialidases generated BV-like glycan phenotypes. As well, exposure of cultured vaginal epithelial cells to recombinant *Gardnerella* sialidase led to desialylation of glycans and induction of pathways regulating cell death, differentiation, and inflammatory responses. These data provide evidence that the vaginal epithelial cells exhibit an altered glycan landscape in BV and suggest that BV-associated glycosidic enzymes may lead to changes in epithelial gene transcription that promote cell turnover and regulate responses towards the resident microbiome. Given the widespread roles of sialoglycans in biology and disease, these findings may point to a shared epithelial pathophysiology underlying the many adverse outcomes associated with BV.

One Sentence Summary:

Resident bacteria damage carbohydrates on vaginal epithelial cell surfaces.

Introduction

Resident vaginal bacteria play key roles in women’s sexual and reproductive health (1, 2). Abundant *Lactobacillus* in the vagina is associated with lower risks of gynecologic and obstetric health complications (3–6). In bacterial vaginosis (BV) there are fewer lactobacilli, and the vagina is instead colonized by diverse anerobic bacteria such as *Gardnerella* (7–11). BV is associated with pregnancy loss (12, 13), preterm birth (14–16), postsurgical infections (17), pelvic inflammatory disease (18–20), and sexually transmitted infections including chlamydia, gonorrhea, and HIV (21–23). Despite the broad impact of BV on gynecologic, sexual, and reproductive health, current treatments are inadequate and recurrences are frequent (24).

In BV, vaginal bacteria live in close proximity to the epithelium (10, 25–27). Epithelial cells covered in bacteria, known as ‘clue cells’, are a major criterion for clinical diagnosis of BV (28, 29). Fluorescence *in situ* hybridization studies have identified some of the attached bacteria, which include *Gardnerella*, *Atopobium, Mobiluncus,* and BVAB1–3 (10, 25, 30, 31). BV is associated with increased shedding of vaginal epithelial cells (VECs) from the superficial layers into the lumen (32, 33). The bacteria-studded, ruffled, and damaged appearance of these exfoliated cells in BV (33) supports the hypothesis that bacterial attack on the epithelium might contribute to the wide-ranging health risks posed by BV.

Mammalian epithelial cells are densely coated with carbohydrate chains (glycans) (34–36) that are often the first point of contact for microbes at mucosal sites (37). The cellular glycan coat or glycocalyx can provide physical protection from pathogens (38, 39), mediate host-microbe interactions (40), and regulate immunity (41–44). Host glycans can be modified in many human diseases (45, 46), including infectious diseases caused by viruses and bacteria (47). Prior studies have investigated glycans in human cervicovaginal fluid (48–54). However, epithelial glycans in the vagina are poorly defined and their functions (and dysfunctions) remain elusive.

Several lines of evidence suggest that the biology of carbohydrates may be important in the underlying physiology of BV. Amounts of carbohydrate-degrading enzymes (glycosidases) in vaginal fluid are higher in women with BV compared to those without BV (52, 55–57). Moreover, vaginal fluids with high concentrations of mucin-degrading enzymes were more likely to exhibit low viscosity (58). One of the most prominent glycoside hydrolases in BV is sialidase, which is not only diagnostic for BV (55, 59) but also associated with adverse pregnancy outcomes including pregnancy loss, preterm birth, and placental infection (56, 60, 61). Sialidases liberate sialic acids from their outermost position on mammalian glycans. Bacteria expressing sialidase activity have been isolated from women with BV (55, 62), suggesting vaginal sialidases are likely of bacterial origin. Prior studies have further shown that sialidases from the common BV bacterium *Gardnerella* can remove sialic acids from mammalian glycoproteins such as immunoglobulins and mucins (62, 63). Consistent with this observation, mucus secretions of women with BV have higher amounts of liberated sialic acid (61,63) and an overall depletion of sialic acids attached to glycans (62). Together the evidence suggests that vaginal bacteria in BV are capable of degrading host glycans.

Here we pursued the hypothesis that the vaginal epithelial glycocalyx is an unappreciated target for bacterial hydrolytic enzymes in BV. We use several complementary methods to elucidate the landscape of glycans on the surfaces of epithelial cells derived from human vaginal specimens. These data provide a blue-print for vaginal epithelial *N*- and *O*-glycosylation. Evidence is presented in support of three interpretations: that epithelial glycans sustain hydrolytic damage in BV, that BV-like glycan phenotypes can be emulated by treatment of ’normal’ VECs with recombinant *Gardnerella* sialidases, and that changes in cultured VEC gene expression in response to sialidase may shed light on epithelial cell behaviors in BV.

Results

Sialic acids are depleted from the vaginal glycocalyx in BV

Sialic acids are terminal sugars decorating mammalian glycans. The most abundant sialic acid in humans is *N*-acetylneuraminic acid (Neu5Ac) (42). To evaluate the effect of BV on VEC sialoglycans we performed analysis of sialic acid on the cell surface by lectin confocal microscopy. Primary epithelial cells were isolated from vaginal swab eluates from women with BV (Nugent score 7–10) or without BV (Nugent score 0–3, referred to as ‘normal’ or ‘No BV’ hereafter). These samples were previously collected as part of the contraceptive CHOICE project, which enrolled adult women in the St. Louis area who were sexually active and in search of (free) contraception (see the Materials and Methods).

By design, our study did not perform any matching of samples in the Nugent-defined BV or No BV groups, nor did we undertake efforts to exclude samples from individuals with sexually transmitted infection. Consistent with prior reports, individuals with BV were more likely to be Black, and had other factors previously linked with BV (see table S1 and paragraph two of the Discussion). BV-status was determined using Nugent's scoring method for analysis of Gram-stained slides of vaginal specimens (64). Sialidase activity was measured in each vaginal specimen by incubating the swab eluate with fluorogenic substrate Neu5Ac-4-methyl umbelliferone (4MUSia). Initial investigation of the epithelial surface sialylation performed in specimens without BV revealed prominent binding of the *Maackia amurensis* lectin-II (MAL-II) (Fig. 1A), which recognizes terminal α2–3-linked sialic acid residues (Neu5Acα2–3Gallβ1–3GalNAc) (65). In contrast, eight of nine BV specimens with high sialidase activity (rate of 4MUSia hydrolysis > 0.1 μM/min) showed negligible MAL-II staining, suggesting extensive depletion of epithelial α2–3-linked sialic acids in BV. In some BV specimens with low sialidase activity, evident MAL-II binding suggested that sialic acid depletion was related to the presence of sialidases in vaginal fluids (Fig. 1A). Specificity was confirmed by pretreating No BV VECs with exogenous sialidase from *Arthrobacter ureafaciens* (*A.u.* sialidase), which eliminated MAL-II binding (fig. S1A). Similarly, MAL-II binding was lower in blots of protein extracts from BV VECs (fig. S1B), compared to No BV VECs, which was further reduced or eliminated upon treatment with *A.u.* sialidase. In agreement with previous studies (55, 57), we found sialidase activity was significantly higher ($P < 0.0001$) in samples from women with BV compared to without BV (Fig. 1B).

The repertoire of glycans on mammalian cell surfaces varies from tissue to tissue and its characterization can be complicated by branching and extensive heterogeneity (66). Two abundant glycan types modify proteins on mammalian surfaces. *O*-linked glycans are found on serine or threonine residues, whereas *N*-linked glycans are attached to asparagine residues. To investigate the impact of BV on terminal sialic acids decorating *N*-glycans, we blotted protein extracts of VECs using *Sambucus nigra* agglutinin (SNA) that binds to sialic acid residues α2–6-linked to galactose (Neu5Acα2–6Gal) (fig. S2A). Fewer bands and less overall SNA binding was observed in BV compared to 'normal' specimens (fig. S2C). In parallel, we also blotted protein extracts of VECs using *Erythrina cristagalli* agglutinin (ECA), which binds to galactose (Galβ1–4GlcNAc) underlying sialic acids (fig. S2A). ECA binding was only detected in the protein extracts of No BV specimens when treated with exogenous *A.u.* sialidase (AUS) (fig. S2D), indicating that the galactose residues were capped by sialic acids in 'normal' VECs. In contrast, ECA binding was observed in BV specimens (fig. S2D) regardless of sialidase treatment. In control samples treated with PNGase F (fig. S2B), both ECA and SNA binding were either reduced or not detected (fig. S2C, S2D), confirming these lectins recognize epitopes in VEC *N*-glycans. Together these data point towards depletion of α2–6 linked sialic acids from VEC glycans.

To quantitatively assess the degree of sialylation on *N*- and *O*-glycans, epithelial cells were pooled from multiple specimens to yield sufficient material for analysis. Glycans were released from equal amounts of extracted protein for each condition. *N*-glycans were released with PNGase F under denaturing conditions, whereas *O*-glycans were released using reductive beta-elimination. Subsequently, sialic acids were released from glycans by

mild acid hydrolysis, fluorescent derivatized using 1,2-diamino-4,5-methylenedioxybenzene (DMB), and quantified by reverse-phase chromatography by comparison to synthetic standards. Biochemical measurements of sialic acids (Neu5Ac) in these preparations revealed that the extent of sialylation in BV specimens was ~4.5-fold lower on *N*-glycans, and ~9-fold lower on *O*-glycans, compared to No BV specimens (Figs. 1C, D). As a control, pooled VECs from women without BV were pretreated with exogenous *A.u.* sialidase and washed to remove liberated sialic acid prior to lysate preparation, revealing BV-like *N*- and *O*-glycans with low amounts of sialic acid. These results, together with the lectin analysis, strongly suggest that α2–3- and α2–6-linked sialic acids are depleted from the epithelial glycans in individuals with BV.

Depletion of negatively charged *N*-linked glycans on epithelial cells in BV

To further characterize epithelial *N*-glycans, we employed anion exchange chromatography to separate neutral and negatively charged glycans. This analysis distinguishes between different types of *N*-glycans [such as high mannose (neutral) or mono-, bi-, tri- and tetra-antennary sialylated glycans]. *N*-glycans were isolated from VEC protein extracts using PNGase F, labelled with 2-amino benzamide (2-AB), and analyzed by high-performance anion exchange chromatography (HPAEC) with fluorimetric detection (Fig. 2A). *N*-glycan standards isolated from the glycoproteins RNase B and bovine fetuin were analyzed in parallel, illustrating a clear separation between neutral and charged glycans. Neutral *N*-glycan structures were abundant in all samples. However, peaks corresponding to negatively charged *N*-glycans were smaller and fewer among glycans derived from BV compared to No BV specimens (Fig. 2B). When glycans derived from No BV specimens were experimentally treated with sialidase, most of the negatively charged (sialylated) peaks disappeared, and the *N*-glycans adopted a BV-like profile (Fig. 2C). These results demonstrate that sialylated epithelial *N*-glycans are found at substantially lower amounts in BV.

To further resolve potential changes in *N*-glycan structures we examined the composition of *N*-glycans, derived from the VECs of an individual specimen of No BV and BV, using high resolution LC-MS/MS (67). Epithelial *N*-glycans obtained from a specimen without BV had a prominent signal arising from a di-sialylated biantennary *N*-glycan (Fig. 2D and fig. S3). Masses corresponding to sialylated bi-antennary *N*-glycans were seen at much lower intensities in the BV sample, which instead had prominent peaks for the corresponding de-sialylated *N*-glycans with terminally exposed galactose (Fig. 2D and fig. S3). Additionally, we observed that fucosylated *N*-glycans terminating in galactose were highly abundant in the BV specimen (Fig. 2D and fig. S3), plausibly due to the loss of sialic acid residues from the parent sialofucosylated structures observed on ‘normal’ epithelial cells in women without BV (fig. S3). In contrast, in the BV specimen, we did not observe glycan masses corresponding to these complex structures in which both antennae have a terminal GlcNAc that is not capped by Gal. This result, together with ECA lectin analysis (fig. S2D), argues against extensive, processive exo-deglycosylation and provide further resolution of the sialylated glycans that are depleted from epithelial cells in BV.

O-glycans of human VECs

In women without BV, our measurements of sialic acid amounts suggested that the vaginal glycocalyx contains abundant sialylated *O*-glycans. To identify the relevant *O*-glycan structures of VECs, mass spectrometric (MS) analysis was performed on permethylated epithelial *O*-glycans derived from pooled VECs of women without BV. The most commonly found *O*-glycans in mammals are the mucin type *O*-glycans (68). Biosynthesis of mucin type *O*-glycosylation is initiated by addition of an alpha-linked *N*-acetylgalactosamine (α-GalNAc) residue to a serine or threonine residue in the peptide backbone (68, 69). Subsequently, the core GalNAc can be extended with other sugars to form several different core structures. For example, the core-2 structures are generated by the addition of a β1–6 linked *N*-acetylglucosamine (GlcNAc) to the GalNAc in core 1. Analysis of 'normal' VEC *O*-glycans using matrix-assisted laser desorption/ionization-time of flight mass spectrometry (MALDI-TOF) revealed that the vaginal glycocalyx contains multiple sialylated *O*-glycan structures. Among these, we observed a small fraction of di-sialylated core 1 structures (Galβ1–3GalNAc-Ser/Thr) with m/z 1256, and relatively high abundance of differentially sialylated and fucosylated core 2 structures (Fig. 3A). Specifically, in 'normal' VEC *O*-glycans, the highest intensity peak was consistent with a di-sialylated and fucosylated core 2 ion with m/z 1879, containing a potential sialyl Lewis X (sLeX, also known as CD15s) on one antenna. To further verify the presence of a Lewis X (CD15) structure (fig. S4A) we used an anti-Lewis X antibody to probe VECs isolated from No BV vaginal specimens, with or without prior treatment with exogenous sialidase (*A.u.* sialidase). Confocal imaging (fig. S4B) and flow cytometry (fig. S4C) analysis confirmed the presence of Lewis X containing glycans on VECs of women without BV. A substantial increase in anti-Lewis X binding was observed when VECs were treated with *A.u.* sialidase (fig. S4C), suggesting that most of the Lewis X antigens present on 'normal' VECs were sialylated.

O-glycan structures of VECs derived from No BV and BV specimens were assigned by tandem MS (MS/MS) analysis (70) of selected precursor ions using a linear ion trap mass spectrometer (LTQ-MS). The MS/MS fragmentation spectra of permethylated *O*-glycans derived from No BV VECs contained molecular ions characteristic of core 1 and fucosylated core 2 *O*-glycans (fig. S5). Fragmentation of the sialylated *O*-glycan precursor ion with m/z 1256 yielded a Y-ion corresponding to sialylated T-antigen (Neu5Ac-Galβ1–3GalNAc-Ser/Thr, m/z 881) and a Z-ion corresponding to sialyl-Tn antigen (Neu5Ac2–6GalNAc-Ser/Thr, m/z 659) with much lower intensity (fig. S5A), confirming a core 1 structure. Similarly, fragmentation of the most abundant di-sialylated core 2 ion (m/z 1879) yielded daughter ions with m/z 1504, 1673, 1282 and 1129 confirming a branched glycan (fig. S5A).

Analysis of *O*-glycans isolated from pooled VECs, derived from BV-positive vaginal specimens, using MALDI-TOF MS revealed that the relative intensity of sialyl Lewis X containing core 2 ion (m/z 1879) was less than < 30% (Fig. 3B), which was much lower compared to its relative intensity (>80%) in No BV *O*-glycans. It is plausible that depletion of sialic acids from epithelial cell *O*-glycans results in the lower relative abundance of core 2 ion (m/z 1879) we observed in BV. Corroborating these data, we also observed a concurrent higher intensity of a core 2 ion lacking sialic acids (m/z 983) in BV *O*-glycans (Fig. 3B). In support of this assignment, MS/MS analysis (by LTQ-MS) of the most abundant *O*-glycan

ion (m/z 983) yielded daughter ions with m/z 747 (Z-ion), 520 (Y-ion, T-antigen), and 486 (B-ion, LacNAc), confirming the presence of a core 2 structure with LacNAc on one antenna and T-antigen on the other (fig. S5A). Further MS/MS analysis of the precursor ion with m/z 1157 yielded several fucose-containing daughter ions with m/z 921 (most abundant, Fucose{Gal-GlcNAc}), 694 (Fucose-Gal-GalNAc with reducing end) and 660 (Fucose{Gal-GlcNAc}), suggesting the presence of multiple fucosylated glycoforms lacking terminal sialic acid residues (fig. S5B).

To determine if these changes in the molecular ion intensity were due to de-sialylation of glycans, we analyzed *O*-glycans isolated from pooled VECs that were derived from women without BV and pretreated with *A.u.* sialidase (Fig. 3C). We found that the MALDI-TOF *O*-glycoprofile of sialidase-pretreated No BV VECs was similar to that obtained from women with BV. The highest peak in the *O*-glycans of sialidase pretreated samples corresponded to the de-sialylated core 2 ion (m/z 983), whereas the relative intensity of molecular ion m/z 1879 (sialic acid containing core 2 ion) was less than 30% (Fig. 3C). To further characterize *O*-glycan structures, we performed linkage analysis of charged *O*-glycans from No BV VECs confirming the presence of 3-GalNAc-itol, 3,6-GalNAc-itol, and 4-GlcNAc (fig. S6 and table S2), which was consistent with core 1 and core 2 *O*-glycan structures detected in MS/MS analysis (fig. S5). Detection of both 3-linked Gal and 6-linked Gal was consistent with α2–3 as well as α2–6 sialic acid decoration, as shown in earlier lectin blots and confocal imaging experiments. Additionally, the presence of terminal fucose and 3,4-GlcNAc supports the presence of Lewis antigen(s) on No BV VECs.

We also resolved *O*-glycan composition from VECs obtained from individual specimens (one No BV and one BV) using high resolution LC-MS/MS (67). In the absence of BV, approximately 80% of the *O*-glycans were sialylated (20% sialylated; 62% sialofucosylated) (fig. S7). In BV, ~50% of *O*-glycans were sialylated (16% sialylated, 35% sialofucosylated), with correspondingly higher intensities of galactose terminating glycans (~48% neutral + fucosylated). Taken together, these data provide the first comprehensive blueprint of the vaginal epithelial *O*-glycan landscape in reproductive age women.

Exposure of carbohydrates underlying sialic acids on VECs in BV

Sialic acids are most often present at the terminal position of glycans and can protect the underlying sugars from degradation by glycoside hydrolases (71, 72). In both *N*- and *O*-linked glycans, sialic acids often cap galactose (Gal) residues attached to GlcNAc or GalNAc. To determine if terminal Gal residues are accessible on the vaginal cell surface, we used peanut agglutinin (PNA), a lectin that recognizes T antigen (Galβ1–3GalNAc) when the Gal is not capped by sialic acids (Fig. 4A) (73). To distinguish if the PNA epitopes on vaginal epithelial surfaces were masked by sialic acids or simply not present at all, PNA binding was compared between cells from the same sample that were either untreated or pretreated with exogenous sialidase (*A.u.* sialidase). We observed minimal PNA binding (red) to untreated VECs in No BV samples (Fig. 4B). However, a substantial increase in PNA binding was observed when the VECs from the same sample were treated with sialidase. This suggested that the PNA epitope is present on No BV VECs but is typically masked by sialic acids. In contrast, cells from BV-positive specimens showed

considerable PNA binding even in the absence of sialidase treatment (Fig. 4B). Furthermore, PNA binding to VECs from women with BV did not increase upon sialidase treatment, suggesting that the PNA epitopes were largely not masked by sialic acids in BV. These data corroborate our analytical observation of hypo-sialylated epithelial glycans in BV, and strongly support the conclusion that uncapped Gal residues (as part of the T antigen) are present on the VEC surface in BV. Control experiments confirmed PNA selectivity and ruled out non-specific binding (fig. S8). As expected, PNA binding to sialidase-treated epithelial cells from BV-positive samples could be out-competed with excess lactose (Galβ1–4-Glc), but not with sucralose. Notably, counter-staining with DAPI (blue) revealed that the cells from BV-positive individuals had large numbers of bacteria covering their surfaces (fig. S9), and appeared to be pink/purple in color (Fig. 4C), similar to 'clue cells' observed in BV-positive samples by wet mount microscopy (28). In contrast, the *A.u.* sialidase treated cells from BV-negative samples had few adherent bacteria and hence appeared to be red upon PNA binding.

To further quantify the amount of cell surface galactose exposure on epithelial cells from individuals with and without BV, we used flow cytometry to measure PNA binding to VECs. Analysis of the same gated population of cells (fig. S10A) from BV and No BV samples showed that PNA binding to cells from BV-positive samples was higher compared to the No BV controls in the absence of any exogenous sialidase treatment (Fig. 4D). In contrast, epithelial cells from all samples were labeled with PNA after sialidase treatment. The extent of exposure of Gal residues in each group was calculated as the percentage ratio of PNA binding to cells in absence versus presence of treatment with *A.u.* sialidase. Using this metric, VECs from BV-positive samples had a significantly higher ($P < 0.0001$) portion of uncapped Galβ1–3GalNAc (PNA recognized) epitopes compared to No BV cells (Fig. 4E).

As noted previously (55), samples from individual BV-positive samples also had higher sialidase activity (fig. S10B). Correlation analysis using data from individual un-pooled samples revealed a direct relationship between the amount of detectable sialidase activity and the percentage of exposed galactose on the epithelial cell surface in individuals with BV (fig. S10C), analogous to the results presented in Fig 1A. Furthermore, in most BV samples with high sialidase activity (relative sialidase activity >0.5) more than 90% of galactose was exposed on the VEC glycans. Notably, in a small proportion of BV samples, high galactose exposure (>60%) was also observed on cells from vaginal swabs with very low or no detectable sialidase activity. This suggested that the phenotype of higher PNA binding to VECs may be a more sensitive indicator of BV compared to sialidase, persisting even when sialidase activity is not detectable. Based on the distribution of data from samples in both patient groups, we considered 60% galactose exposure as a threshold and compared the data to the Nugent's method (64). Using this small sample set, we found that epithelial cell-PNA-binding analysis had a specificity of 100% and sensitivity of 80% (Fig. 4E), suggesting this may be a useful area for diagnostic development.

Gardnerella sialidases hydrolyze sialic acids from VECs and generate BV-like glycan phenotypes

So far, we have used a commercially available recombinant sialidase from *A. ureafaciens* as a control, to demonstrate the potential impact of exogenous sialidase on glycan phenotypes. Next, we tested if the more relevant sialidases from *Gardnerella*, often one of the most abundant microbes in BV (11), could generate BV-like glycan phenotypes.

Specifically, we investigated if *Gardnerella* sialidases degrade glycan components on the epithelial surface, hydrolyzing sialic acids and yielding underlying Galβ1–3GalNAc epitopes recognized by PNA. Briefly, pooled VECs from individuals without BV were treated with commercial *A.u.* sialidase or recombinant enzymes from *Gardnerella* (NanH2 or NanH3) (63). In parallel, a proportion of VECs from the same pool were mock-treated using material derived from identically prepared *E. coli* containing an empty vector. Sialic acids hydrolyzed from epithelial cells were measured by fluorescent derivatization and HPLC, as described earlier for analysis of sialic acid associated with *N*- and *O*-glycans. Cells were also subjected to PNA staining. The data show that *Gardnerella* sialidases NanH2 and NanH3 were adept at removing sialic acids from epithelial cells (Fig. 5A), revealing PNA-reactive underlying Galβ1–3GalNAc epitopes as measured by flow cytometry (Fig. 5B). Consistent with findings in Fig. 4, BV samples analyzed in parallel had high galactose exposure (PNA binding) that could not be further increased with treatment by any of the sialidases (Fig. 5C). Confocal imaging of PNA-stained cells further underscored the generation of a BV-like phenotype when No BV samples were treated with *Gardnerella* sialidase (Fig. 5D). As observed earlier, cells from BV-positive samples appeared pink/purple in coloration due to adherent bacteria that were stained blue with DAPI, whereas sialidase treated cells from BV-negative samples appeared red. Overall, these data suggest that sialidases produced by BV-associated bacteria such as *Gardnerella* result in degradation of vaginal epithelial sialoglycans.

Reduced glycocalyx staining in BV specimens is phenocopied using recombinant *Gardnerella* sialidase

Last, we used classical methods to assess the impact of BV on the appearance of the VEC glycocalyx. VECs were prepared for transmission electron microscopy (TEM) by staining with ruthenium red and osmium tetroxide to visualize the glycocalyx (74, 75). To determine if glycocalyx staining was affected by BV-status or experimental treatments, we evaluated the extent of the glycocalyx that was apparent to observers on VECs by blinded scoring of TEM images. Micrographs were collected by a single blinded microscopist and scored by three blinded observers using the scoring method described in fig. S11A, from zero (“none visible”) to four (“highly abundant”). Specimens without BV had a fuzzy layer of glycocalyx protruding from the ‘normal’ VEC membrane (Fig. 6A, and figs. S11B, S12A), as previously observed in other mammals (76). In comparison, the appearance (staining) of the glycocalyx was diminished in BV specimens (Figs. 6B, and figs. S11B, S12B). In parallel, we analyzed of images of ‘normal’ VECs from women without BV that were treated with recombinant purified *Gardnerella* sialidase (NanH2) (63). Here, we observed that the appearance of glycocalyx of ‘normal’ VECs was significantly diminished

in appearance upon treatment with *Gardnerella* sialidase (Fig. 6C and fig. S11B), similar to the glycocalyx of BV-VECs.

Among the epithelial cell images from 'normal' specimens (No BV), that were not treated with sialidase, 95% were scored as having a visible glycocalyx (38/40 score >1) (Fig. 6D). In contrast, blinded scoring indicated that epithelial cells of BV specimens had no visible glycocalyx in micrographs ~63% of the time (19/30 had a 0 score from all three observers) (Fig. 6D). Notably, sialidase treatment led to significantly diminished ($P < 0.0001$) staining of the glycocalyx (Fig. 6E), similar to what was observed with BV-positive VECs. For example, whereas the untreated group had a score of 2 or greater in 32/40 (~80%) images, cells treated with *Gardnerella* sialidase had a glycocalyx score less than two in 29/30 (~97%) images (Fig. 6E). Ruthenium red is a polycationic dye that stains acidic polysaccharides and therefore can facilitate visualization of anionic structures (containing sialic acids or other negatively charged glycans) on cell surfaces in conjunction with osmium tetroxide, which attaches to vicinal dihydroxylated molecules. The sensitivity of this staining method to *Gardnerella* sialidase suggests that sialic acids are the major contributors to the negative charge of the VEC surface. Hence, depletion of sialic acids from the cell surface results in a failure to detect the glycocalyx in BV-VECs, even though the underlying glycans are evidently present as confirmed by lectin staining and mass spectrometric analysis of earlier specimens in this study.

TEM images of VECs (Fig. 6 and figs. S11, S12) had heterogenous intracellular compartments, with some micrographs displaying a threaded or striated appearance and others a more globular appearance. To decipher the relationship of this phenotype, if any, with BV-status, blinded observers scored TEM images as 1 if greater than 50% of the intracellular compartment had a threaded appearance and scored the images as 0 otherwise. The analysis revealed that the threaded appearance of the intracellular compartment is specific to BV specimens and 'normal' (No BV) VECs treated with recombinant *Gardnerella* sialidase (fig. S11C).

Gardnerella sialidase alters regulation of cell migration, death, and inflammatory pathways in VECs

To investigate the biological impact of modified host glycans in BV, we characterized the initial transcriptional responses by treating the VK2 cells with recombinant sialidase from *Gardnerella* (NanH2). We purified recombinant NanH2 (rNanH2) using Clear coli cells (*E. coli* with detoxified LPS) (Fig. 7A). A parallel preparation was made from Clear coli cells containing empty vector. Treatment of VK2 cells with rNanH2 resulted in the release of sialic acids (Fig. 7B). RNA-seq analysis of VK2 cells treated with rNanH2 revealed that 23 genes were significantly up-regulated and 3 genes were significantly down-regulated (adjusted P value < 0.05) after 1 h of exposure to *Gardnerella* sialidase (Fig. 7C, 7D and table S3). Some of these were transcription factors, such as *KLF4* and *EGR1*, that are known to regulate interactions of bacterial pathogens with host-epithelial cells (77, 78). Differentially expressed genes were also analyzed for functional enrichment to determine the affected gene ontology biological processes (GOBP). Pathways enriched after one hour treatment with rNanH2 (adj. p value < 9.0e−04, after multiple testing correction)

were primarily related to cell migration, including adhesion, locomotion, movement, morphogenesis, proliferation, and tissue development (Table 1). Thus, even a relatively short exposure of VECs to *Gardnerella* sialidase activity triggers an alteration of the transcription profile when compared to cells treated with vector control.

In VK2 cells subjected to longer treatment (2 h) with rNanH2, genes that were significantly up-regulated (adjusted P value < 0.05) included TNF Alpha induced protein 3 (*TNFAIP3*, ~5 fold-change) and Nuclear factor-kappa B (NF-κB) Inhibitor Alpha (*NFKBIA*, ~3 fold-change) (Fig. 7C, 7E and table S3). The protein encoded by *TNFAIP3*, known as A20, acts in concert with NF-κB signaling to regulate cell survival and define balance between pro-apoptotic or anti-apoptotic pathways in a cell type dependent manner (79, 80). Consistent with this, pathways enriched at this timepoint included programmed cell death, regulation of cell death, immune response, TLR signaling pathway, and response to molecules of bacterial origin (Table 1). This suggests that sialoglycan degradation on the vaginal epithelium may be an important determinant of the apoptosis, cell exfoliation, and inflammatory responses observed in BV (32, 33, 81).

Discussion

Epithelial surface glycans help maintain homeostasis within mucosal biomes (82–86). Thus, a full understanding of the physiology of the vaginal epithelium requires detailed knowledge of the structure and functions of glycans at the epithelial cell surface. Here we elucidate the vaginal epithelial glycan landscape using cells isolated directly from human vaginal specimens. Analytic approaches revealed prominent sialoglycans on the epithelial cell surface and protein extracts of VECs from ‘normal’ specimens without BV (Nugent score 0–3), containing both α2–3 linked and α2–6 linked sialic acids, as is often seen on other mammalian mucosal surfaces (87, 88). In contrast, cells from women with BV (Nugent score 7–10) displayed fewer sialylated epithelial *N*- and *O*-glycans, with loss of sialic acids in both linkages. Earlier studies have reported the presence of other glycosidic enzymes in BV, such as beta-galactosidases, assayed using synthetic small molecule substrates (52). However, the genetic basis of this activity or the natural substrates for such enzymes were unknown. Here, we show using multiple lectins and mass spectrometric analysis that galactose terminating *N*- and *O*-glycans are more prominent in the epithelial glycocalyx of BV-positive women. Collectively, the data presented here suggest widespread removal of sialic acids from cellular *N*- and *O*-glycans that does not appear to be accompanied by a similar digestion of underlying residues. Together, the data illustrate that VEC glycans undergo conspicuous changes in the setting of BV.

In these experiments, samples were selected based on BV-status (Nugent 0–3 for negative and 7–10 for positive) from a larger cohort without introducing any strategies to balance the groups for potential confounders. Although not examined here, other studies have found correlates between BV and psychosocial stress (89, 90). One limitation is that we cannot formally rule out contributions by potentially confounding factors to the glycan landscape. For example, other biochemical studies have suggested fine regulation of glycans during the menstrual cycle in the endocervical mucus (50, 91). However, studies that have looked at both the microbiome and the secreted reproductive tract glycans together, suggested that the

microbiome has a decisive effect (53). Similarly, the concordance we observed between microbes, BV-status, enzyme activities, and the corresponding degradation of glycan structures strongly argues for a causal relationship between these phenotypes associated with VECs. The finding that *Gardnerella* sialidase acts on epithelial cells to emulate BV-like glycan phenotypes lends further credence to a causal relationship.

Several lines of evidence strongly suggest that damage to vaginal epithelial glycans is mediated by extrinsic effects of microbiota-derived enzymes in BV. First, sialidase activity in BV specimens corresponds with the presence of sialidase-producing bacterial species, including *Gardnerella* (55, 62). Second, the depletion of α2–3- and α2–6-linked sialic acids from epithelial glycans (shown here) is consistent with the breadth of substrates cleaved by BV sialidases, whether assayed in BV specimens using exogenous substrates like immunoglobulins (57), live *Gardnerella* cultures (62, 63), or using recombinant *Gardnerella* enzymes (NanH2 or NanH3) (63). Third, BV specimens contain substantially higher amounts of liberated (free) sialic acid even though there are lower amounts of (bound) sialoglycans (62, 92). This is consistent with *in vitro* observations that strains of *Gardnerella* that express sialidase activity liberate (free) sialic acid into the extracellular space, followed by overall depletion of both free and bound sialic acids (62). Last, our data show that recombinant *Gardnerella* sialidases liberate sialic acids from ‘normal’ epithelial cells, resulting in a BV-like epithelial surface (as evidenced by the appearance of terminal Gal and visibly diminished glycocalyces).

Changes to the glycocalyx may have diverse physiological consequences that could help reveal the pathological mechanisms of BV. From a physical standpoint, the acidic functional groups of sialylated glycans confer a negative charge to the cell surface. Alterations in the organization and net charge contributed by sialic acids are understood to contribute to pathophysiologies of the blood and renal systems (93–97) and could likewise impair functions of the vaginal epithelium. In addition to physical effects, the liberation of sialic acids from host cell glycans can provide opportunities for bacterial nutrient acquisition and colonization, including some opportunistic pathogens lacking sialidase activity (62, 98–100). De-sialylation may also modify glycan-receptor interactions influencing microbial adhesion, inflammatory responses, or other aspects of host-microbe biology. Viral, bacterial, or eukaryotic pathogens linked with BV may use lectins to exploit the newly accessible glycan epitopes (for example exposed Gal residues). For example, *Fusobacterium nucleatum* encodes multiple galactose-recognizing adhesins (101, 102) and colonizes women with BV more often than women without (9, 14). The relative absence of sialic acids and exposure of galactose on the BV epithelium could therefore lead to improved colonization by *F. nucleatum* or other potential pathogens linked with BV. Changes in the glycan landscape of the cervicovaginal epithelium may also impact recognition by endogenous lectin receptors of the host. For example, the sialic acid-binding Siglecs and the galactose-binding Galectins are expressed in the female reproductive tract (103–105) and are known to modulate cellular responses such as inflammatory activation and cell death in other physiological settings (42, 106–110).

Our RNAseq results are consistent with earlier findings that epithelial cells in BV undergo apoptosis (33) and might help explain why there are higher numbers of exfoliated

epithelial cells in BV and in mice vaginally infected with *Gardnerella (32, 33, 81)*. In particular, sialidase action on the vaginal epithelium led to the induction of *EGR1*, *NFKBIA* and *TNFAIP3*. These factors regulate signaling for cell growth and death directed by glycosylated receptors on the cell surface (111, 112), and earlier studies report that sialylation impacts signaling through EGFR1 (113, 114) and TNFR1 (115). Together, the evidence suggests that BV-bacteria may modify host sialoglycans to regulate cell growth and death pathways to generate a more suitable niche.

This study has several limitations. First, analysis of human vaginal glycans does not allow for direct interpretation of the causes of structural changes and there were several potential demographic confounders among the studied groups of individuals. Despite providing multiple lines of evidence for extrinsic bacterial effects on the glycocalyx, the current experiments do not formally rule out the possibility that intrinsic host glycosyltransferases or glycosidases could also be dysregulated in BV. On the other hand, a reductionist approach using cultured epithelial cells and recombinant *Gardnerella* sialidase could be misleading because it cannot replicate the complex physiology of the vagina. Likewise, studies of the role(s) of sialidase in epithelial apoptosis and the generation of inflammatory processes etc. is limited by a lack of genetic systems in *Gardnerella* and few experimental models of BV capable of revealing BV-like characteristics.

Overall, these findings provide new insights into the biology of BV, which is poorly understood despite its widespread impact on sexual, reproductive, and perinatal health. Even though available antibiotics reduce the symptoms of BV in the short term, recurrences occur in most women within 12 months of treatment (116). Future work should investigate if long-term efficacy after treatment is contingent upon rehabilitating damaged glycans. If so, the restoration of normal glycosylation might be a valuable test of treatment success or a target for drug development. Additional studies should leverage relevant experimental models and clinical cohorts to understand how specific changes to the glycocalyx may contribute to cellular signaling and function, and how these relate to the biological and clinical facets of BV.

Materials and Methods

Study design

This study was designed to investigate the impact of vaginal microbiota (optimal and non-optimal) on the host epithelial cell glycans in women with and without BV. Previously collected vaginal swabs leftover from the inaugural Contraceptive CHOICE Project (CHOICE), a prospective cohort study that enrolled women in the St. Louis (Missouri, USA) region (117), were used in this study. CHOICE received informed consent in writing from all participants at enrollment, as well as permission to use vaginal samples for future studies. CHOICE inclusion criteria included reported sexual activity in the past six months or anticipated sexual activity with a male partner; willingness to try a new contraceptive method; and the desire to prevent pregnancy for at least 12 months. Exclusion criteria were ages outside the 14–45-year age range and a history of tubal ligation or hysterectomy, as previously described (117). A total of 258 specimens from individual women were used in the experiments reported here. Inclusion criteria for this sub-study were an available

specimen Nugent score of 0–3 (No BV) or 7–10 (BV). The sub-study with CHOICE specimens was originally reviewed and approved by the Institutional Review Board at Washington University School of Medicine (IRB ID # 201108155).

Samples represent a cross-section of women from the same approximate (2-year) collection time window of CHOICE enrollment. Demographic characteristics of the participants in this sub study are presented in table S1. We did not exclude specimens from women who were pregnant, menstruating, or those with sexually transmitted infections. Samples were either tested as individual specimens or pooled to reach the minimum material required for the experiment (see detailed rationale for pooling in supplementary materials). Sample sizes were estimated based on previous experiments quantifying sialic acid in vaginal specimens.

Two specimens from the Urogenital Community (UC) Bank project (one from one individual without BV and one with BV), were used for the experiments reported here (LC-MS analysis of *N*- and *O*-glycans) according to Washington University in Saint Louis IRB-approved protocol (#20170412; PI, Amanda Lewis). Written informed consent was obtained, participants were enrolled, and swabs were collected as described earlier (100). For additional information related to selection and processing of these two specimens see the supplementary materials.

VECs isolated from the vaginal swabs were used for characterizing the epithelial glycan landscape in women with and without BV. Cells from individual specimens, or pooled VECs from multiple specimens in the same group, were used for analysis by lectin staining, liquid chromatography, and mass-spectrometry to gather a blueprint of glycan structures present in VECs of women with and without BV. Independent observers were blinded to the BV-status of the sample during evaluation. Further, the cells derived from these specimens were also used to evaluate the hydrolytic effects of BV-bacteria associated glycosidic enzymes (such as sialidases), on the vaginal epithelial glycans.

Vaginal specimen collection, handling, and Nugent scoring for the CHOICE project

Upon enrollment, women were given a double-headed rayon swab inside a collection tube (Starplex Scientific Inc.) and were instructed on a self-collection protocol. Immediately after collection, a single technician rolled one swab onto a glass slide. Remaining swab material was stored at −80 °C. Slides were heat-fixed, Gram stained, and subjected to Nugent scoring. In general, this scoring system uses weighted quantitation of bacterial morphotype to reflect the overall character of vaginal bacteria present (64). Nugent scores are reflected on a scale of 0 to 10 combined from three components for each sample: a score of 0–4 reflecting the presence of rod-shaped Gram-positive lactobacilli where 0 indicates highest numbers; a score of 0–4 reflecting the presence of Gram-negative and Gram-variable morphotypes where 4 indicates the highest numbers; and a score of 0–2 reflecting the presence of curved rods. A sample with score of 0–3 was considered not to have BV (without BV/No BV, 'normal'), and a sample with score of 7–10 was considered BV-positive.

Processing of specimens from the CHOICE project

For all analyses of VECs, vaginal swabs were selected based on Nugent score from reproductive age women with BV (Nugent score 7–10) or without BV (Nugent score 0–3). No attempts were made to exclude swabs from women who had clinical indications of sexually transmitted infection. Vaginal swabs were stored at −80 °C until processed further. Swabs were cut to approximately ~3.5–4.0 cm and enclosed in a cryotube. Swabs were removed from the freezer onto wet ice and eluted by immersing in 1 mL of 100 mM sodium acetate (pH 5.5, swab elution buffer (SEB) incubated in an ice bucket for 1 h followed by shaking at 500 rpm, using a IKA MS 3 digital, for 10 min at room temperature. The individual swab eluates were transferred to microcentrifuge tubes and kept on ice. To check for sialidase activity, 50 μL of eluate was resuspended and transferred to 96 well round bottom black polypropylene plates. Sialidase assay was performed as described in the supplementary materials. In parallel, a second elution was performed by again immersing the same swabs in 1 mL of SEB in individual cryo tubes, followed immediately by shaking at 500 rpm for 10 min at room temperature. Cells were isolated from the swab eluates by centrifugation at 1000 × g for 5 min at room temperature after each elution step. Microscopic examination of the isolated cells confirmed the morphology as polygonal squamous epithelial cells with a diameter of 50–70 μm and no other morphologies were observed.

Statistical analysis

GraphPad Prism 9.0 software was used for all statistical analyses presented. The statistical tests used to analyze each set of data, number of specimens, and the number of replicates or independent experiments is indicated in the figure legends. For non-parametric analyses, we used the two-tailed unpaired Mann-Whitney U test or Dunn’s test for multiple comparisons. For treatments done on batches of the same original sample (paired datasets), results were analyzed using Wilcoxon matched-pairs sign rank test. For categorical variables, we used a two-sided Fisher’s exact test. $P < 0.05$ was considered significant.

Supplementary Material

Refer to Web version on PubMed Central for supplementary material.

Acknowledgements

We thank Andrea Verhagen, Christy Armstrong, and Siyu Chen for technical contributions and assistance. We are grateful to Dr. Wandy L. Beatty and the staff of the Molecular Microbiology Imaging Facility at Washington University in St. Louis (MO, USA) for assistance with TEM, and to Dr. Sulabha Argade and Dr. Mousumi Paulchakrabarti at the GlycoAnalytics Core, Glycobiology Research and Training Center, University of California San Diego (CA, USA) for expert technical assistance with glycan characterization. We also acknowledge Jennifer Reed (formerly Bick) for technical assistance with Nugent scoring of CHOICE clinical specimens. Last, we thank all of the participants who generously shared samples used in this study.

Funding

This work was funded by the National Institute of Allergy and Infectious Diseases (R01 AI114635 to ALL and WGL, R01 AI127554 to WGL), the Burroughs Wellcome Fund Preterm Birth Initiative (to ALL) and the University of California Glycosciences Consortium for Women’s Health. This publication includes data generated at the UC San Diego IGM Genomics Center utilizing an Illumina NovaSeq 6000 that was purchased with funding from a National Institutes of Health SIG grant (#S10 OD026929). The project described was partially supported by the

National Institutes of Health, Grant UL1TR001442 of Clinical and Translational Science Awards (CTSA) program. The content is solely the responsibility of the authors and does not necessarily represent the official views of the NIH. This work was also supported by the Stephen I. Morse fellowship to K.A. (Department of Molecular Microbiology, Washington University in St. Louis, MO, USA). Funding for the Contraceptive CHOICE Project was provided by an anonymous foundation.

Data and materials availability

All data associated with this study are available in the supplementary materials or have been deposited in the National Center for Biotechnology Information Sequence Read Archive (SRA, BioProject ID PRJNA982281). Codes related to the RNA seq analysis are available in the repository ucsd-ccbb/VK2-vaginal-epithelial-cell-RNA-seq-analysis with zenodo DOI link- DOI: 10.5281/zenodo.8422984. Raw data from figures are available in data file S1 and *N*-glycan LC-MS/MS data are in data file S2. Requests for materials (such as plasmids) should be made to the corresponding authors.

References and Notes

1. Callahan BJ, DiGiulio DB, Goltsman DSA, Sun CL, Costello EK, Jeganathan P, Biggio JR, Wong RJ, Druzin ML, Shaw GM, Stevenson DK, Holmes SP, Relman DA, Replication and refinement of a vaginal microbial signature of preterm birth in two racially distinct cohorts of US women. Proc Natl Acad Sci U S A 114, 9966–9971 (2017). [PubMed: 28847941]
2. Hillier SL, Bernstein KT, Aral S, A Review of the Challenges and Complexities in the Diagnosis, Etiology, Epidemiology, and Pathogenesis of Pelvic Inflammatory Disease. J Infect Dis 224, S23–S28 (2021). [PubMed: 34396398]
3. Witkin SS, Linhares IM, Why do lactobacilli dominate the human vaginal microbiota? BJOG 124, 606–611 (2017). [PubMed: 28224747]
4. Kroon SJ, Ravel J, Huston WM, Cervicovaginal microbiota, women's health, and reproductive outcomes. Fertil Steril 110, 327–336 (2018). [PubMed: 30098679]
5. Amabebe E, Anumba DOC, The Vaginal Microenvironment: The Physiologic Role of Lactobacilli. Front Med (Lausanne) 5, 181 (2018). [PubMed: 29951482]
6. Al-Memar M, Bobdiwala S, Fourie H, Mannino R, Lee YS, Smith A, Marchesi JR, Timmerman D, Bourne T, Bennett PR, MacIntyre DA, The association between vaginal bacterial composition and miscarriage: a nested case-control study. BJOG 127, 264–274 (2020). [PubMed: 31573753]
7. Piot P, Van Dyck E, Godts P, Vanderheyden J, The vaginal microbial flora in non-specific vaginitis. Eur J Clin Microbiol 1, 301–306 (1982). [PubMed: 6985215]
8. Hill GB, Eschenbach DA, Holmes KK, Bacteriology of the vagina. Scand J Urol Nephrol Suppl 86, 23–39 (1984). [PubMed: 6399406]
9. Hillier SL, Krohn MA, Rabe LK, Klebanoff SJ, Eschenbach DA, The normal vaginal flora, H2O2-producing lactobacilli, and bacterial vaginosis in pregnant women. Clin Infect Dis 16 Suppl 4, S273–281 (1993). [PubMed: 8324131]
10. Fredricks DN, Fiedler TL, Marrazzo JM, Molecular identification of bacteria associated with bacterial vaginosis. N Engl J Med 353, 1899–1911 (2005). [PubMed: 16267321]
11. Ravel J, Gajer P, Abdo Z, Schneider GM, Koenig SS, McCulle SL, Karlebach S, Gorle R, Russell J, Tacket CO, Brotman RM, Davis CC, Ault K, Peralta L, Forney LJ, Vaginal microbiome of reproductive-age women. Proc Natl Acad Sci U S A 108 Suppl 1, 4680–4687 (2011). [PubMed: 20534435]
12. Hay PE, Lamont RF, Taylor-Robinson D, Morgan DJ, Ison C, Pearson J, Abnormal bacterial colonisation of the genital tract and subsequent preterm delivery and late miscarriage. BMJ 308, 295–298 (1994). [PubMed: 8124116]
13. Leitich H, Brunbauer M, Bodner-Adler B, Kaider A, Egarter C, Husslein P, Antibiotic treatment of bacterial vaginosis in pregnancy: a meta-analysis. Am J Obstet Gynecol 188, 752–758 (2003). [PubMed: 12634652]

14. Holst E, Goffeng AR, Andersch B, Bacterial vaginosis and vaginal microorganisms in idiopathic premature labor and association with pregnancy outcome. J Clin Microbiol 32, 176–186 (1994). [PubMed: 8126176]
15. Hillier SL, Nugent RP, Eschenbach DA, Krohn MA, Gibbs RS, Martin DH, Cotch MF, Edelman R, Pastorek JG 2nd, Rao AV, et al. , Association between bacterial vaginosis and preterm delivery of a low-birth-weight infant. The Vaginal Infections and Prematurity Study Group. N Engl J Med 333, 1737–1742 (1995). [PubMed: 7491137]
16. Fettweis JM, Serrano MG, Brooks JP, Edwards DJ, Girerd PH, Parikh HI, Huang B, Arodz TJ, Edupuganti L, Glascock AL, Xu J, Jimenez NR, Vivadelli SC, Fong SS, Sheth NU, Jean S, Lee V, Bokhari YA, Lara AM, Mistry SD, Duckworth RA 3rd, Bradley SP, Koparde VN, Orenda XV, Milton SH, Rozycki SK, Matveyev AV, Wright ML, Huzurbazar SV, Jackson EM, Smirnova E, Korlach J, Tsai YC, Dickinson MR, Brooks JL, Drake JI, Chaffin DO, Sexton AL, Gravett MG, Rubens CE, Wijesooriya NR, Hendricks-Munoz KD, Jefferson KK, Strauss JF 3rd, Buck GA, The vaginal microbiome and preterm birth. Nat Med 25, 1012–1021 (2019). [PubMed: 31142849]
17. Soper DE, Bacterial vaginosis and surgical site infections. Am J Obstet Gynecol 222, 219–223 (2020). [PubMed: 31499057]
18. Wiesenfeld HC, Hillier SL, Krohn MA, Amortegui AJ, Heine RP, Landers DV, Sweet RL, Lower genital tract infection and endometritis: insight into subclinical pelvic inflammatory disease. Obstet Gynecol 100, 456–463 (2002). [PubMed: 12220764]
19. Taylor BD, Darville T, Haggerty CL, Does bacterial vaginosis cause pelvic inflammatory disease? Sex Transm Dis 40, 117–122 (2013). [PubMed: 23324974]
20. Ravel J, Moreno I, Simon C, Bacterial vaginosis and its association with infertility, endometritis, and pelvic inflammatory disease. Am J Obstet Gynecol 224, 251–257 (2021). [PubMed: 33091407]
21. Brotman RM, Klebanoff MA, Nansel TR, Yu KF, Andrews WW, Zhang J, Schwebke JR, Bacterial vaginosis assessed by gram stain and diminished colonization resistance to incident gonococcal, chlamydial, and trichomonal genital infection. J Infect Dis 202, 1907–1915 (2010). [PubMed: 21067371]
22. Bautista CT, Wurapa EK, Sateren WB, Morris SM, Hollingsworth BP, Sanchez JL, Association of Bacterial Vaginosis With *Chlamydia* and *Gonorrhea* Among Women in the U.S. Army. Am J Prev Med 52, 632–639 (2017). [PubMed: 27816380]
23. Atashili J, Poole C, Ndumbe PM, Adimora AA, Smith JS, Bacterial vaginosis and HIV acquisition: a meta-analysis of published studies. AIDS 22, 1493–1501 (2008). [PubMed: 18614873]
24. Vodstrcil LA, Muzny CA, Plummer EL, Sobel JD, Bradshaw CS, Bacterial vaginosis: drivers of recurrence and challenges and opportunities in partner treatment. BMC Med 19, 194 (2021). [PubMed: 34470644]
25. Cook RL, Reid G, Pond DG, Schmitt CA, Sobel JD, Clue cells in bacterial vaginosis: immunofluorescent identification of the adherent gram-negative bacteria as *Gardnerella vaginalis*. J Infect Dis 160, 490–496 (1989). [PubMed: 2668431]
26. Gardner HL, Dukes CD, *Haemophilus vaginalis* vaginitis: a newly defined specific infection previously classified non-specific vaginitis. Am J Obstet Gynecol 69, 962–976 (1955). [PubMed: 14361525]
27. Swidsinski A, Mendling W, Loening-Baucke V, Ladhoff A, Swidsinski S, Hale LP, Lochs H, Adherent biofilms in bacterial vaginosis. Obstet Gynecol 106, 1013–1023 (2005). [PubMed: 16260520]
28. Amsel R, Totten PA, Spiegel CA, Chen KC, Eschenbach D, Holmes KK, Nonspecific vaginitis. Diagnostic criteria and microbial and epidemiologic associations. Am J Med 74, 14–22 (1983). [PubMed: 6600371]
29. Schwebke JR, Marrazzo J, Beelen AP, Sobel JD, A Phase 3, Multicenter, Randomized, Double-Blind, Vehicle-Controlled Study Evaluating the Safety and Efficacy of Metronidazole Vaginal Gel 1.3% in the Treatment of Bacterial Vaginosis. Sex Transm Dis 42, 376–381 (2015). [PubMed: 26222750]
30. Srinivasan S, Morgan MT, Liu C, Matsen FA, Hoffman NG, Fiedler TL, Agnew KJ, Marrazzo JM, Fredricks DN, More than meets the eye: associations of vaginal bacteria with gram stain

morphotypes using molecular phylogenetic analysis. PLoS One 8, e78633 (2013). [PubMed: 24302980]

31. Hardy L, Jespers V, Dahchour N, Mwambarangwe L, Musengamana V, Vaneechoutte M, Crucitti T, Unravelling the Bacterial Vaginosis-Associated Biofilm: A Multiplex *Gardnerella vaginalis* and *Atopobium vaginae* Fluorescence In Situ Hybridization Assay Using Peptide Nucleic Acid Probes. PLoS One 10, e0136658 (2015). [PubMed: 26305575]
32. Amegashie CP, Gilbert NM, Peipert JF, Allsworth JE, Lewis WG, Lewis AL, Relationship between nugent score and vaginal epithelial exfoliation. PLoS One 12, e0177797 (2017). [PubMed: 28562623]
33. Roselletti E, Sabbatini S, Perito S, Mencacci A, Vecchiarelli A, Monari C, Apoptosis of vaginal epithelial cells in clinical samples from women with diagnosed bacterial vaginosis. Sci Rep 10, 1978 (2020). [PubMed: 32029862]
34. Ceralli F, Familiari G, Marinozzi G, Muccioli-Casadei D, The glycocalyx of the epithelial cells of the colon, observed in normal and ulcerous colitic conditions. Experientia 32, 1542–1544 (1976). [PubMed: 1021443]
35. Levin S, Richter WR, Ultrastructure of cell surface coat (glycocalyx) in rat urinary bladder epithelium. Cell Tissue Res 158, 281–283 (1975). [PubMed: 48426]
36. Martins Mde F, Bairos VA, Glycocalyx of lung epithelial cells. Int Rev Cytol 216, 131–173 (2002). [PubMed: 12049207]
37. Poole J, Day CJ, von Itzstein M, Paton JC, Jennings MP, Glycointeractions in bacterial pathogenesis. Nat Rev Microbiol 16, 440–452 (2018). [PubMed: 29674747]
38. Cohen M, Zhang XQ, Senaati HP, Chen HW, Varki NM, Schooley RT, Gagneux P, Influenza A penetrates host mucus by cleaving sialic acids with neuraminidase. Virol J 10, 321 (2013). [PubMed: 24261589]
39. Argueso P, Woodward AM, AbuSamra DB, The Epithelial Cell Glycocalyx in Ocular Surface Infection. Front Immunol 12, 729260 (2021). [PubMed: 34497615]
40. Arabyan N, Park D, Foutouhi S, Weis AM, Huang BC, Williams CC, Desai P, Shah J, Jeannotte R, Kong N, Lebrilla CB, Weimer BC, *Salmonella* Degrades the Host Glycocalyx Leading to Altered Infection and Glycan Remodeling. Sci Rep 6, 29525 (2016). [PubMed: 27389966]
41. Cobb BA, Kasper DL, Coming of age: carbohydrates and immunity. Eur J Immunol 35, 352–356 (2005). [PubMed: 15682450]
42. Varki A, Gagneux P, Multifarious roles of sialic acids in immunity. Ann N Y Acad Sci 1253, 16–36 (2012). [PubMed: 22524423]
43. Dias AM, Pereira MS, Padrao NA, Alves I, Marcos-Pinto R, Lago P, Pinho SS, Glycans as critical regulators of gut immunity in homeostasis and disease. Cell Immunol 333, 9–18 (2018). [PubMed: 30049413]
44. Brazil JC, Parkos CA, Finding the sweet spot: glycosylation mediated regulation of intestinal inflammation. Mucosal Immunol, (2021).
45. Pinho SS, Reis CA, Glycosylation in cancer: mechanisms and clinical implications. Nat Rev Cancer 15, 540–555 (2015). [PubMed: 26289314]
46. Reily C, Stewart TJ, Renfrow MB, Novak J, Glycosylation in health and disease. Nat Rev Nephrol 15, 346–366 (2019). [PubMed: 30858582]
47. Lewis AL, Lewis WG, Host sialoglycans and bacterial sialidases: a mucosal perspective. Cell Microbiol 14, 1174–1182 (2012). [PubMed: 22519819]
48. Yurewicz EC, Matsuura F, Moghissi KS, Structural characterization of neutral oligosaccharides of human midcycle cervical mucin. J Biol Chem 257, 2314–2322 (1982). [PubMed: 6277894]
49. Yurewicz EC, Matsuura F, Moghissi KS, Structural studies of sialylated oligosaccharides of human midcycle cervical mucin. J Biol Chem 262, 4733–4739 (1987). [PubMed: 3558366]
50. Andersch-Bjorkman Y, Thomsson KA, Holmen Larsson JM, Ekerhovd E, Hansson GC, Large scale identification of proteins, mucins, and their O-glycosylation in the endocervical mucus during the menstrual cycle. Mol Cell Proteomics 6, 708–716 (2007). [PubMed: 17220477]
51. Moncla BJ, Chappell CA, Debo BM, Meyn LA, The Effects of Hormones and Vaginal Microflora on the Glycome of the Female Genital Tract: Cervical-Vaginal Fluid. PLoS One 11, e0158687 (2016). [PubMed: 27437931]

52. Moncla BJ, Chappell CA, Mahal LK, Debo BM, Meyn LA, Hillier SL, Impact of bacterial vaginosis, as assessed by nugent criteria and hormonal status on glycosidases and lectin binding in cervicovaginal lavage samples. PLoS One 10, e0127091 (2015). [PubMed: 26011704]
53. Wang L, Koppolu S, Chappell C, Moncla BJ, Hillier SL, Mahal LK, Studying the effects of reproductive hormones and bacterial vaginosis on the glycome of lavage samples from the cervicovaginal cavity. PLoS One 10, e0127021 (2015). [PubMed: 25993513]
54. Wu G, Grassi P, MacIntyre DA, Molina BG, Sykes L, Kundu S, Hsiao CT, Khoo KH, Bennett PR, Dell A, Haslam SM, N-glycosylation of cervicovaginal fluid reflects microbial community, immune activity, and pregnancy status. Sci Rep 12, 16948 (2022). [PubMed: 36216861]
55. Briselden AM, Moncla BJ, Stevens CE, Hillier SL, Sialidases (neuraminidases) in bacterial vaginosis and bacterial vaginosis-associated microflora. J Clin Microbiol 30, 663–666 (1992). [PubMed: 1551983]
56. Howe L, Wiggins R, Soothill PW, Millar MR, Horner PJ, Corfield AP, Mucinase and sialidase activity of the vaginal microflora: implications for the pathogenesis of preterm labour. Int J STD AIDS 10, 442–447 (1999). [PubMed: 10454178]
57. Lewis WG, Robinson LS, Perry J, Bick JL, Peipert JF, Allsworth JE, Lewis AL, Hydrolysis of secreted sialoglycoprotein immunoglobulin A (IgA) in ex vivo and biochemical models of bacterial vaginosis. J Biol Chem 287, 2079–2089 (2012). [PubMed: 22134918]
58. Olmsted SS, Meyn LA, Rohan LC, Hillier SL, Glycosidase and proteinase activity of anaerobic gram-negative bacteria isolated from women with bacterial vaginosis. Sex Transm Dis 30, 257–261 (2003). [PubMed: 12616147]
59. Kampan NC, Suffian SS, Ithnin NS, Muhammad M, Zakaria SZ, Jamil MA, Evaluation of BV((R)) Blue Test Kit for the diagnosis of bacterial vaginosis. Sex Reprod Healthc 2, 1–5 (2011). [PubMed: 21147452]
60. Zhang X, Xu X, Li J, Li N, Yan T, Ju X, [Relationship between vaginal sialidase bacteria vaginosis and chorioammionitis]. Zhonghua Fu Chan Ke Za Zhi 37, 588–590 (2002). [PubMed: 12487930]
61. Cauci S, Culhane JF, High sialidase levels increase preterm birth risk among women who are bacterial vaginosis-positive in early gestation. Am J Obstet Gynecol 204, 142 e141–149 (2011).
62. Lewis WG, Robinson LS, Gilbert NM, Perry JC, Lewis AL, Degradation, foraging, and depletion of mucus sialoglycans by the vagina-adapted Actinobacterium *Gardnerella vaginalis*. J Biol Chem 288, 12067–12079 (2013). [PubMed: 23479734]
63. Robinson LS, Schwebke J, Lewis WG, Lewis AL, Identification and characterization of NanH2 and NanH3, enzymes responsible for sialidase activity in the vaginal bacterium *Gardnerella vaginalis*. J Biol Chem 294, 5230–5245 (2019). [PubMed: 30723162]
64. Nugent RP, Krohn MA, Hillier SL, Reliability of diagnosing bacterial vaginosis is improved by a standardized method of gram stain interpretation. J Clin Microbiol 29, 297–301 (1991). [PubMed: 1706728]
65. Geisler C, Jarvis DL, Effective glycoanalysis with *Maackia amurensis* lectins requires a clear understanding of their binding specificities. Glycobiology 21, 988–993 (2011). [PubMed: 21863598]
66. Varki A, in Essentials of Glycobiology, Varki A, Cummings RD, Esko JD, Freeze HH, Stanley P, Bertozzi CR, Hart GW, Etzler ME, Eds. (Cold Spring Harbor (NY), 1999).
67. Li Q, Xie Y, Wong M, Barboza M, Lebrilla CB, Comprehensive structural glycomic characterization of the glycocalyxes of cells and tissues. Nat Protoc 15, 2668–2704 (2020). [PubMed: 32681150]
68. Van den Steen P, Rudd PM, Dwek RA, Opdenakker G, Concepts and principles of O-linked glycosylation. Crit Rev Biochem Mol Biol 33, 151–208 (1998). [PubMed: 9673446]
69. Brockhausen I, Stanley P, in Essentials of Glycobiology, Varki A, Cummings RD, Esko JD, Stanley P, Hart GW, Aebi M, Darvill AG, Kinoshita T, Packer NH, Prestegard JH, Schnaar RL, Seeberger PH, Eds. (Cold Spring Harbor (NY), 2015), pp. 113–123.
70. Domon B, Costello CE, A Systematic Nomenclature for Carbohydrate Fragmentations in Fab-Ms Ms Spectra of Glycoconjugates. Glycoconjugate J 5, 397–409 (1988).
71. Hoskins LC, Human enteric population ecology and degradation of gut mucins. Dig Dis Sci 26, 769–772 (1981). [PubMed: 7285743]

72. Yudin AI, Treece CA, Tollner TL, Overstreet JW, Cherr GN, The carbohydrate structure of DEFB126, the major component of the cynomolgus Macaque sperm plasma membrane glycocalyx. J Membr Biol 207, 119–129 (2005). [PubMed: 16550483]
73. Chacko BK, Appukuttan PS, Peanut (Arachis hypogaea) lectin recognizes alpha-linked galactose, but not N-acetyl lactosamine in N-linked oligosaccharide terminals. Int J Biol Macromol 28, 365–371 (2001). [PubMed: 11325423]
74. Luft JH, Fine structures of capillary and endocapillary layer as revealed by ruthenium red. Fed Proc 25, 1773–1783 (1966). [PubMed: 5927412]
75. Fassel TA, Edmiston CE Jr., Ruthenium red and the bacterial glycocalyx. Biotech Histochem 74, 194–212 (1999). [PubMed: 10555860]
76. King BF, Ruthenium red staining of vaginal epithelial cells and adherent bacteria. Anat Rec 212, 41–46 (1985). [PubMed: 2416249]
77. Banerji R, Saroj SD, Early growth response 1 (EGR1) activation in initial stages of host-pathogen interactions. Mol Biol Rep 48, 2935–2943 (2021). [PubMed: 33783681]
78. Zahlten J, Herta T, Kabus C, Steinfeldt M, Kershaw O, Garcia P, Hocke AC, Gruber AD, Hubner RH, Steinicke R, Doehn JM, Suttorp N, Hippenstiel S, Role of Pneumococcal Autolysin for KLF4 Expression and Chemokine Secretion in Lung Epithelium. Am J Respir Cell Mol Biol 53, 544–554 (2015). [PubMed: 25756955]
79. Baichwal VR, Baeuerle PA, Activate NF-kappa B or die? Curr Biol 7, R94–96 (1997). [PubMed: 9081673]
80. Malewicz M, Zeller N, Yilmaz ZB, Weih F, NF kappa B controls the balance between Fas and tumor necrosis factor cell death pathways during T cell receptor-induced apoptosis via the expression of its target gene A20. J Biol Chem 278, 32825–32833 (2003). [PubMed: 12813034]
81. Gilbert NM, Lewis WG, Lewis AL, Clinical features of bacterial vaginosis in a murine model of vaginal infection with *Gardnerella vaginalis*. PLoS One 8, e59539 (2013). [PubMed: 23527214]
82. Pacheco AR, Curtis MM, Ritchie JM, Munera D, Waldor MK, Moreira CG, Sperandio V, Fucose sensing regulates bacterial intestinal colonization. Nature 492, 113–117 (2012). [PubMed: 23160491]
83. Goto Y, Obata T, Kunisawa J, Sato S, Ivanov II, Lamichhane A, Takeyama N, Kamioka M, Sakamoto M, Matsuki T, Setoyama H, Imaoka A, Uematsu S, Akira S, Domino SE, Kulig P, Becher B, Renauld JC, Sasakawa C, Umesaki Y, Benno Y, Kiyono H, Innate lymphoid cells regulate intestinal epithelial cell glycosylation. Science 345, 1254009 (2014). [PubMed: 25214634]
84. Nita-Lazar M, Banerjee A, Feng C, Amin MN, Frieman MB, Chen WH, Cross AS, Wang LX, Vasta GR, Desialylation of airway epithelial cells during influenza virus infection enhances pneumococcal adhesion via galectin binding. Mol Immunol 65, 1–16 (2015). [PubMed: 25597246]
85. Jeffries JL, Jia J, Choi W, Choe S, Miao J, Xu Y, Powell R, Lin J, Kuang Z, Gaskins HR, Lau GW, *Pseudomonas aeruginosa* pyocyanin modulates mucin glycosylation with sialyl-Lewis(x) to increase binding to airway epithelial cells. Mucosal Immunol 9, 1039–1050 (2016). [PubMed: 26555707]
86. Kudelka MR, Stowell SR, Cummings RD, Neish AS, Intestinal epithelial glycosylation in homeostasis and gut microbiota interactions in IBD. Nat Rev Gastroenterol Hepatol 17, 597–617 (2020). [PubMed: 32710014]
87. Arike L, Holmen-Larsson J, Hansson GC, Intestinal Muc2 mucin O-glycosylation is affected by microbiota and regulated by differential expression of glycosyltranferases. Glycobiology 27, 318–328 (2017). [PubMed: 28122822]
88. Shinya K, Ebina M, Yamada S, Ono M, Kasai N, Kawaoka Y, Avian flu: influenza virus receptors in the human airway. Nature 440, 435–436 (2006). [PubMed: 16554799]
89. Paul K, Boutain D, Manhart L, Hitti J, Racial disparity in bacterial vaginosis: the role of socioeconomic status, psychosocial stress, and neighborhood characteristics, and possible implications for preterm birth. Soc Sci Med 67, 824–833 (2008). [PubMed: 18573578]
90. Borgogna JC, Anastario M, Firemoon P, Rink E, Ricker A, Ravel J, Brotman RM, Yeoman CJ, Vaginal microbiota of American Indian women and associations with measures of psychosocial stress. PLoS One 16, e0260813 (2021). [PubMed: 34890405]

91. Reynoso-Prieto M, Takeda M, Prakobphol A, Seidman D, Averbach S, Fisher S, Smith-McCune K, Menstrual cycle-dependent alterations in glycosylation: a roadmap for defining biomarkers of favorable and unfavorable mucus. J Assist Reprod Genet 36, 847–855 (2019). [PubMed: 31073726]
92. Srinivasan S, Morgan MT, Fiedler TL, Djukovic D, Hoffman NG, Raftery D, Marrazzo JM, Fredricks DN, Metabolic signatures of bacterial vaginosis. mBio 6, (2015).
93. Eylar EH, Madoff MA, Brody OV, Oncley JL, The contribution of sialic acid to the surface charge of the erythrocyte. J Biol Chem 237, 1992–2000 (1962). [PubMed: 13891108]
94. Gelberg H, Healy L, Whiteley H, Miller LA, Vimr E, In vivo enzymatic removal of alpha 2-->6-linked sialic acid from the glomerular filtration barrier results in podocyte charge alteration and glomerular injury. Lab Invest 74, 907–920 (1996). [PubMed: 8642786]
95. Hebbel RP, Yamada O, Moldow CF, Jacob HS, White JG, Eaton JW, Abnormal adherence of sickle erythrocytes to cultured vascular endothelium: possible mechanism for microvascular occlusion in sickle cell disease. J Clin Invest 65, 154–160 (1980). [PubMed: 7350195]
96. Niculovic KM, Blume L, Wedekind H, Kats E, Albers I, Groos S, Abeln M, Schmitz J, Beuke E, Brasen JH, Melk A, Schiffer M, Weinhold B, Munster-Kuhnel AK, Podocyte-Specific Sialylation-Deficient Mice Serve as a Model for Human FSGS. J Am Soc Nephrol 30, 1021–1035 (2019). [PubMed: 31040189]
97. Sen P, Ghosh D, Sarkar C, Erythrocytic membrane anionic charge, sialic acid content, and their correlations with urinary glycosaminoglycans in preeclampsia and eclampsia. Scand J Clin Lab Invest 80, 343–347 (2020). [PubMed: 32282269]
98. Vimr ER, Troy FA, Identification of an inducible catabolic system for sialic acids (nan) in Escherichia coli. J Bacteriol 164, 845–853 (1985). [PubMed: 3902799]
99. Agarwal K, Lewis AL, Vaginal sialoglycan foraging by *Gardnerella vaginalis*: mucus barriers as a meal for unwelcome guests? Glycobiology 31, 667–680 (2021). [PubMed: 33825850]
100. Agarwal K, Robinson LS, Aggarwal S, Foster LR, Hernandez-Leyva A, Lin H, Tortelli BA, O'Brien VP, Miller L, Kau AL, Reno H, Gilbert NM, Lewis WG, Lewis AL, Glycan cross-feeding supports mutualism between *Fusobacterium* and the vaginal microbiota. PLoS Biol 18, e3000788 (2020). [PubMed: 32841232]
101. Coppenhagen-Glazer S, Sol A, Abed J, Naor R, Zhang X, Han YW, Bachrach G, Fap2 of *Fusobacterium nucleatum* is a galactose-inhibitable adhesin involved in coaggregation, cell adhesion, and preterm birth. Infect Immun 83, 1104–1113 (2015). [PubMed: 25561710]
102. Wu C, Chen YW, Scheible M, Chang C, Wittchen M, Lee JH, Luong TT, Tiner BL, Tauch A, Das A, Ton-That H, Genetic and molecular determinants of polymicrobial interactions in *Fusobacterium nucleatum*. Proc Natl Acad Sci U S A 118, (2021).
103. Okumura CY, Baum LG, Johnson PJ, Galectin-1 on cervical epithelial cells is a receptor for the sexually transmitted human parasite Trichomonas vaginalis. Cell Microbiol 10, 2078–2090 (2008). [PubMed: 18637021]
104. Fichorova RN, Yamamoto HS, Fashemi T, Foley E, Ryan S, Beatty N, Dawood H, Hayes GR, St-Pierre G, Sato S, Singh BN, *Trichomonas vaginalis* Lipophosphoglycan Exploits Binding to Galectin-1 and -3 to Modulate Epithelial Immunity. J Biol Chem 291, 998–1013 (2016). [PubMed: 26589797]
105. Tecle E, Reynoso HS, Wang R, Gagneux P, The female reproductive tract contains multiple innate sialic acid-binding immunoglobulin-like lectins (Siglecs) that facilitate sperm survival. J Biol Chem 294, 11910–11919 (2019). [PubMed: 31201275]
106. Hernandez JD, Baum LG, Ah, sweet mystery of death! Galectins and control of cell fate. Glycobiology 12, 127R–136R (2002).
107. Garner OB, Baum LG, Galectin-glycan lattices regulate cell-surface glycoprotein organization and signalling. Biochem Soc Trans 36, 1472–1477 (2008). [PubMed: 19021578]
108. Rabinovich GA, Croci DO, Regulatory circuits mediated by lectin-glycan interactions in autoimmunity and cancer. Immunity 36, 322–335 (2012). [PubMed: 22444630]
109. Baum LG, Garner OB, Schaefer K, Lee B, Microbe-Host Interactions are Positively and Negatively Regulated by Galectin-Glycan Interactions. Front Immunol 5, 284 (2014). [PubMed: 24995007]

110. Colomb F, Giron LB, Trbojevic-Akmacic I, Lauc G, Abdel-Mohsen M, Breaking the Glyco-Code of HIV Persistence and Immunopathogenesis. Curr HIV/AIDS Rep 16, 151–168 (2019). [PubMed: 30707400]
111. He KL, Ting AT, A20 inhibits tumor necrosis factor (TNF) alpha-induced apoptosis by disrupting recruitment of TRADD and RIP to the TNF receptor 1 complex in Jurkat T cells. Mol Cell Biol 22, 6034–6045 (2002). [PubMed: 12167698]
112. Maegawa M, Arao T, Yokote H, Matsumoto K, Kudo K, Tanaka K, Kaneda H, Fujita Y, Ito F, Nishio K, EGFR mutation up-regulates EGR1 expression through the ERK pathway. Anticancer Res 29, 1111–1117 (2009). [PubMed: 19414352]
113. Britain CM, Bhalerao N, Silva AD, Chakraborty A, Buchsbaum DJ, Crowley MR, Crossman DK, Edwards YJK, Bellis SL, Glycosyltransferase ST6Gal-I promotes the epithelial to mesenchymal transition in pancreatic cancer cells. J Biol Chem 296, 100034 (2021). [PubMed: 33148698]
114. Britain CM, Holdbrooks AT, Anderson JC, Willey CD, Bellis SL, Sialylation of EGFR by the ST6Gal-I sialyltransferase promotes EGFR activation and resistance to gefitinib-mediated cell death. J Ovarian Res 11, 12 (2018). [PubMed: 29402301]
115. Holdbrooks AT, Ankenbauer KE, Hwang J, Bellis SL, Regulation of inflammatory signaling by the ST6Gal-I sialyltransferase. PLoS One 15, e0241850 (2020). [PubMed: 33166339]
116. Bradshaw CS, Morton AN, Hocking J, Garland SM, Morris MB, Moss LM, Horvath LB, Kuzevska I, Fairley CK, High recurrence rates of bacterial vaginosis over the course of 12 months after oral metronidazole therapy and factors associated with recurrence. J Infect Dis 193, 1478–1486 (2006). [PubMed: 16652274]
117. Secura GM, Allsworth JE, Madden T, Mullersman JL, Peipert JF, The Contraceptive CHOICE Project: reducing barriers to long-acting reversible contraception. Am J Obstet Gynecol 203, 115 e111–117 (2010).
118. Sutton-Smith M, Dell A, Analysis of Carbohydrates/Glycoproteins by Mass Spectrometry. Cell Biology *(*Third *Edition),* Celis JE, Ed. (2006), pp. 415–425.
119. Hara S, Takemori Y, Yamaguchi M, Nakamura M, Ohkura Y, Fluorometric high-performance liquid chromatography of *N*-acetyl- and *N*-glycolylneuraminic acids and its application to their microdetermination in human and animal sera, glycoproteins, and glycolipids. Anal Biochem 164, 138–145 (1987). [PubMed: 3674364]
120. Bigge JC, Patel TP, Bruce JA, Goulding PN, Charles SM, Parekh RB, Nonselective and Efficient Fluorescent Labeling of Glycans Using 2-Amino Benzamide and Anthranilic Acid. Anal Biochem 230, 229–238 (1995). [PubMed: 7503412]
121. Dell A, Reason AJ, Khoo KH, Panico M, McDowell RA, Morris HR, Mass spectrometry of carbohydrate-containing biopolymers. Methods Enzymol 230, 108–132 (1994). [PubMed: 8139492]
122. Ceroni A, Dell A, Haslam SM, The GlycanBuilder: a fast, intuitive and flexible software tool for building and displaying glycan structures. Source Code Biol Med 2, 3 (2007). [PubMed: 17683623]
123. Ceroni A, Maass K, Geyer H, Geyer R, Dell A, Haslam SM, GlycoWorkbench: a tool for the computer-assisted annotation of mass spectra of glycans. J Proteome Res 7, 1650–1659 (2008). [PubMed: 18311910]
124. Choudhury B, Carlson RW, Goldberg JB, Characterization of the lipopolysaccharide from a wbjE mutant of the serogroup O11 *Pseudomonas aeruginosa* strain, PA103. Carbohydr Res 343, 238–248 (2008). [PubMed: 18039536]
125. Albersheim P, Nevins DJ, English PD, Karr A, A method for the analysis of sugars in plant cell-wall polysaccharides by gas-liquid chromatography. Carbohydr Res 5, 340–345 (1967).
126. Bjorndal H, Hellerqvist CG, Lindberg B, Svensson S, Gas-Liquid Chromatography and Mass Spectrometry in Methylation Analysis of Polysaccharides. Angew Chem Int Edit 9, 610–619 (1970).
127. Andrews S, FastQC: a quality control tool for high throughput sequence data. (2010) http://www.bioinformatics.babraham.ac.uk/projects/fastqc.
128. Bolger AM, Lohse M, Usadel B, Trimmomatic: a flexible trimmer for Illumina sequence data. Bioinformatics 30, 2114–2120 (2014). [PubMed: 24695404]

129. The Genome Reference Consortium. https://www.ncbi.nlm.nih.gov/grc.

130. Dobin A, Davis CA, Schlesinger F, Drenkow J, Zaleski C, Jha S, Batut P, Chaisson M, Gingeras TR, STAR: ultrafast universal RNA-seq aligner. Bioinformatics 29, 15–21 (2013). [PubMed: 23104886]

131. Li B, Dewey CN, RSEM: accurate transcript quantification from RNA-Seq data with or without a reference genome. BMC Bioinformatics 12, 323 (2011). [PubMed: 21816040]

132. Frankish A, Diekhans M, Ferreira AM, Johnson R, Jungreis I, Loveland J, Mudge JM, Sisu C, Wright J, Armstrong J, et al. , GENCODE reference annotation for the human and mouse genomes. Nucleic Acids Resh 47, D766–D773 (2019).

133. Robinson MD, McCarthy DJ, Smyth GK, edgeR: a Bioconductor package for differential expression analysis of digital gene expression data. Bioinformatics 26, 139–140 (2010). [PubMed: 19910308]

134. Ritchie ME, Phipson B, Wu D, Hu Y, Law CW, Shi W, Smyth GK, limma powers differential expression analyses for RNA-sequencing and microarray studies. Nucleic Acids Res 43, e47 (2015). [PubMed: 25605792]

135. Law CW, Chen Y, Shi W, Smyth GK, voom: Precision weights unlock linear model analysis tools for RNA-seq read counts. Genome Biol 15, R29 (2014). [PubMed: 24485249]

136. Robinson MD, Oshlack A, A scaling normalization method for differential expression analysis of RNA-seq data. Genome Biol 11, R25 (2010). [PubMed: 20196867]

137. Benjamini Y, Hochberg Y, Controlling the false discovery rate: a practical and powerful approach to multiple testing. Journal of the Royal Statistical Society Series B 57, 289–300 (1995).

138. Korotkevich G, Sukhov V, Budin N, Shpak B, Artyomov MN. A. Sergushichev, Fast gene set enrichment analysis. bioRxiv (2019) 10.1101/0660012.

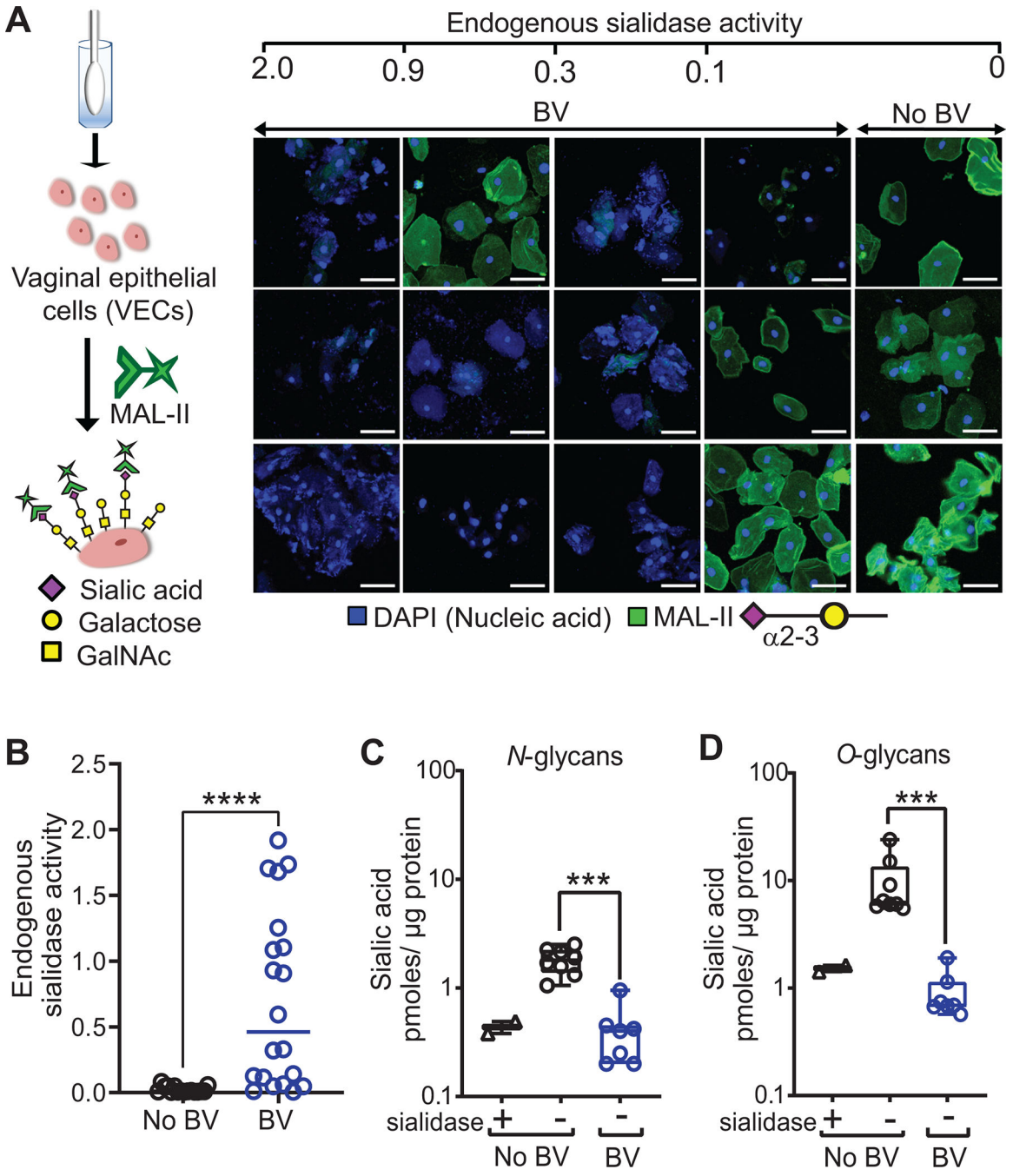

FIG. 1. Depletion of sialic acids from vaginal glycans in women with BV.

(**A**) Left Panel: The schematic shows a summary of cell isolation and lectin staining. Representative mucin-type *O*-glycan structure of sialyl T-antigen, containing alpha1–3 linked sialic acid, is displayed on the cell surface. Right Panel: Representative confocal images of VECs stained with MAL-II lectin (green) recognizing α2–3-linked sialic acids from individual women without BV (n=3) and with BV (n=12). Specimens were compared across varying amounts of endogenous sialidase activity. Nuclei and bacterial cells (blue) are stained with DAPI. Scale bars = 50 μm. (**B**) Quantification of endogenous sialidase activity

in the vaginal swab eluates using the fluorogenic substrate Neu5Ac-4-methyl umbelliferone (4MU-sialic acid). Data shown is the rate of 4MU hydrolysis and the points represent values for individual women (n=16 without BV and n=20 with BV). Data in **A** and **B** is combined from 3 independent experiments. Images shown in **A** are from a subset of specimens used in **B**. (**C** and **D**) Fluorimetric quantification of 1,2-diamino-4,5-methylenedioxybenzene (DMB)-labelled sialic acid (Neu5Ac) in isolated VEC *N*- and *O*-glycans, using reversed-phase chromatography after mild acid hydrolysis. Graph shows sialic acid quantification on glycans derived from protein extracts of pools of VECs from women with BV (Nugent scores 7–10, N=7 pools from a total n=45 specimens, with 5 or 10 specimens in each pool) and without BV (Nugent scores 0–3, No BV, N=8 pools from a total of n=55 specimens, with 5 or 10 specimens in each pool). Glycans derived from No BV VEC pools pretreated with sialidase from *Arthrobacter ureafaciens* were included as a control (N=2 pools with n=10 specimens in each pool). Data in **C** and **D** are from same pools of VECs and were combined from 2 independent experiments. Error bars show standard deviation for each group, Mann–Whitney U test was used. ***P < 0.001, ****P<0.0001. A total of n=151 specimens were used to generate these data. A subset of VEC pools from **C** and **D** were also used for studies reported in Fig. 2, Fig. 3 and table S2. See methods for pooling rationale.

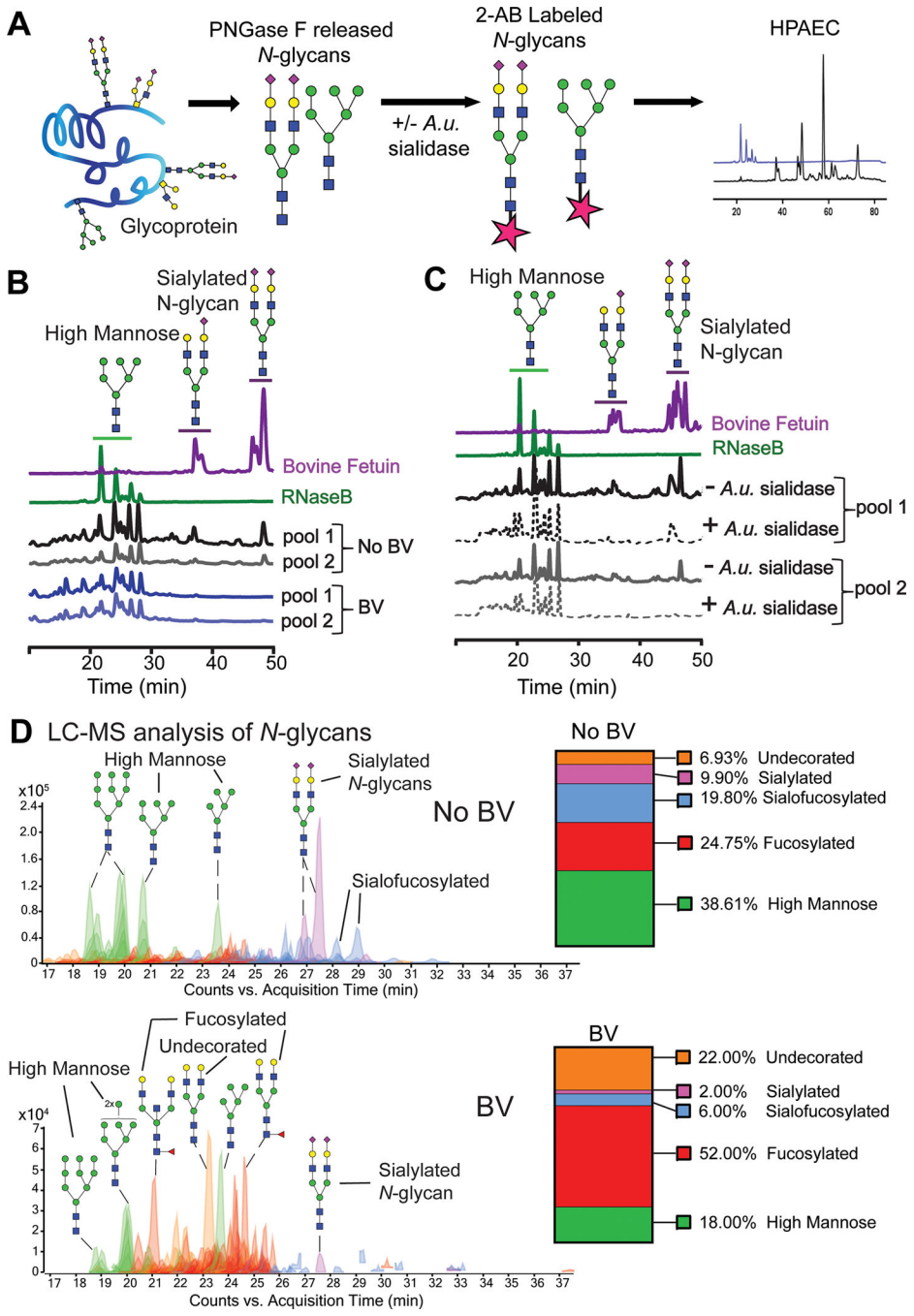

FIG. 2. Sialylated vaginal epithelial *N*-linked glycans are depleted in BV.

(**A**) Schematic for 2-amino benzamide (2AB) profiling of *N*- linked glycans by high performance anion exchange chromatography (HPAEC). Glycans were released using PNGase-F from protein extracts derived from VECs pools and fluorescently labelled with 2-AB prior to analysis by HPAEC. (**B**) HPAEC profiles of 2-AB labeled *N*-glycans derived from protein standards, with well-known glycan structures, RNase B and Bovine Fetuin; 2 pools of No BV VECs (n=10 specimens/pool); and 2 pools of BV VECs (n=10 specimens/pool). (**C**) HPAEC profiles of *N*-glycans derived from RNase B and Bovine Fetuin and

pools of No BV VECs (same VEC pools as used in **B**, n=10 specimens/pool) pretreated with commercially available sialidase (+*A.u.* sialidase, dotted line) or with buffer alone (−*A.u.* sialidase, solid line). *A.u.* sialidase = sialidase from *Arthrobacter ureafaciens.* A total of n=40 specimens (from the CHOICE study) were used to generate data in Fig. 2B and Fig. 2C. VEC pools generated from these specimens were also used for studies reported in Fig. 1C, 1D and Fig. 3. See methods for pooling rationale. (**D**) Chromatograms show probable structures (based on monosaccharide composition) of VEC *N*-glycans derived from one individual woman without BV (upper panel) and with BV (lower panel). Relative abundances of *N*-glycan groups are shown in the bar graph next to the chromatograms. A complete list of *N*-glycan structures and composition, with their relative abundance, for these specimens is provided in data file S2. Structures of different types of *N*-glycans are depicted following the NCBI Symbol Nomenclature for Glycans (yellow circle, galactose; green circle, mannose; blue square, *N*-acetylglucosamine; purple diamond, sialic acid; red triangle, fucose).

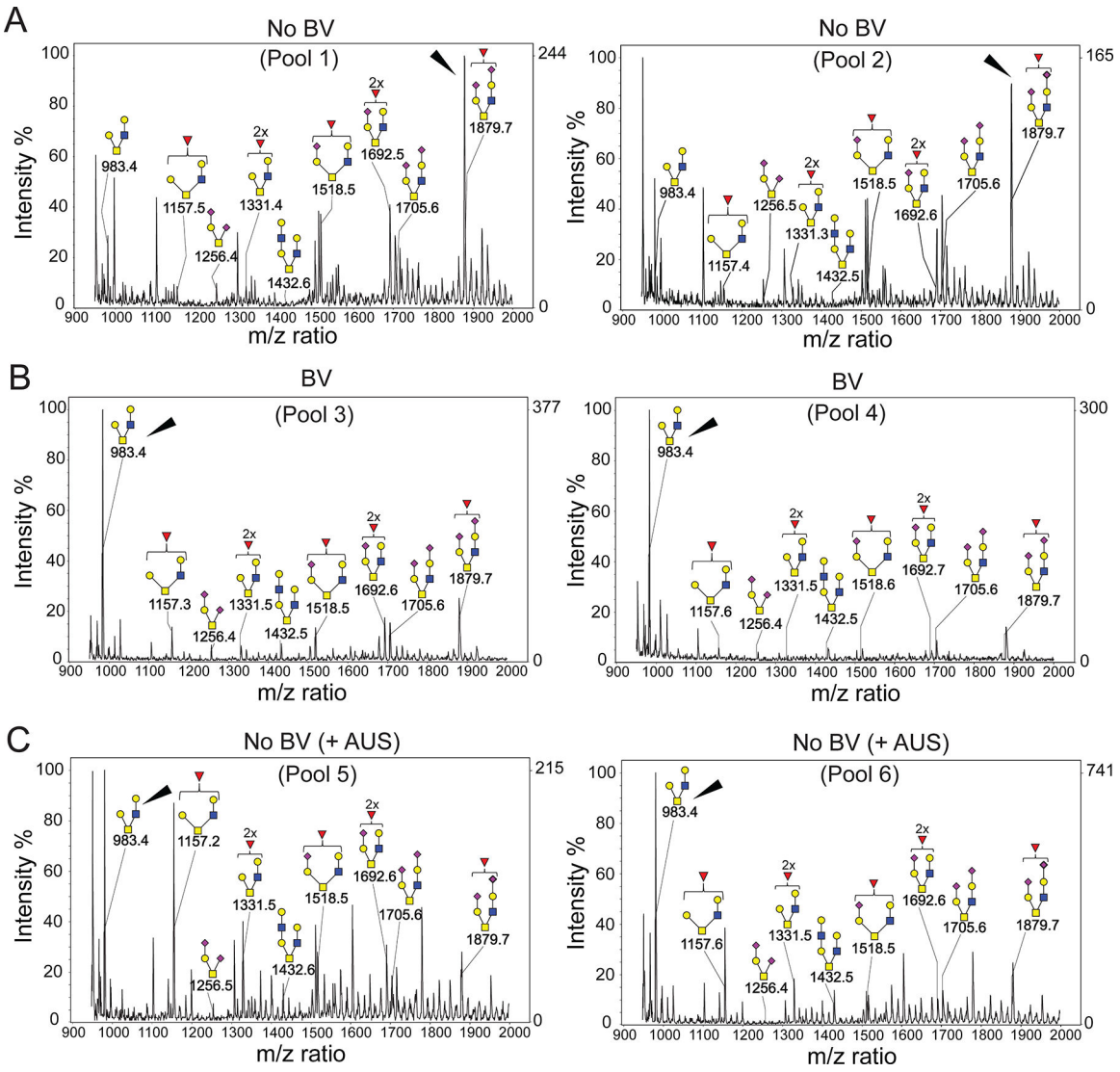

FIG. 3. MALDI-TOF spectra of permethylated *O*-glycans present in vaginal epithelial glycocalyx of individuals with and without BV.

(**A**) Mass spectra shows presence of sialylated core-1 and core-2 glycans in 'normal' (No BV) VECs. (**B**) Asialoglycans dominate (ion m/z = 983) among *O*-glycans derived from BV specimens. (**C**) Pools of VECs from individuals without BV (No BV) pretreated with exogenous sialidase (AUS) show a profile similar to BV specimens. Two different pools were analyzed for each condition (n=10 specimens/pool). Structures of different types of *O*-glycans are depicted following the NCBI Symbol Nomenclature for Glycans (red triangle, fucose; yellow circle, galactose; blue square, *N*-acetylglucosamine; yellow square, *N*-acetylgalactosamine; purple diamond, sialic acid). Arrowheads point to assigned *O*-glycan peaks with highest intensity in the spectra. Data is representative of 3 independent experiments. A total of n=60 specimens were used to generate these data. VEC pools generated from these specimens were also used for studies reported in Fig. 1C, 1D, Fig. 2 and table S2. See methods for pooling rationale.

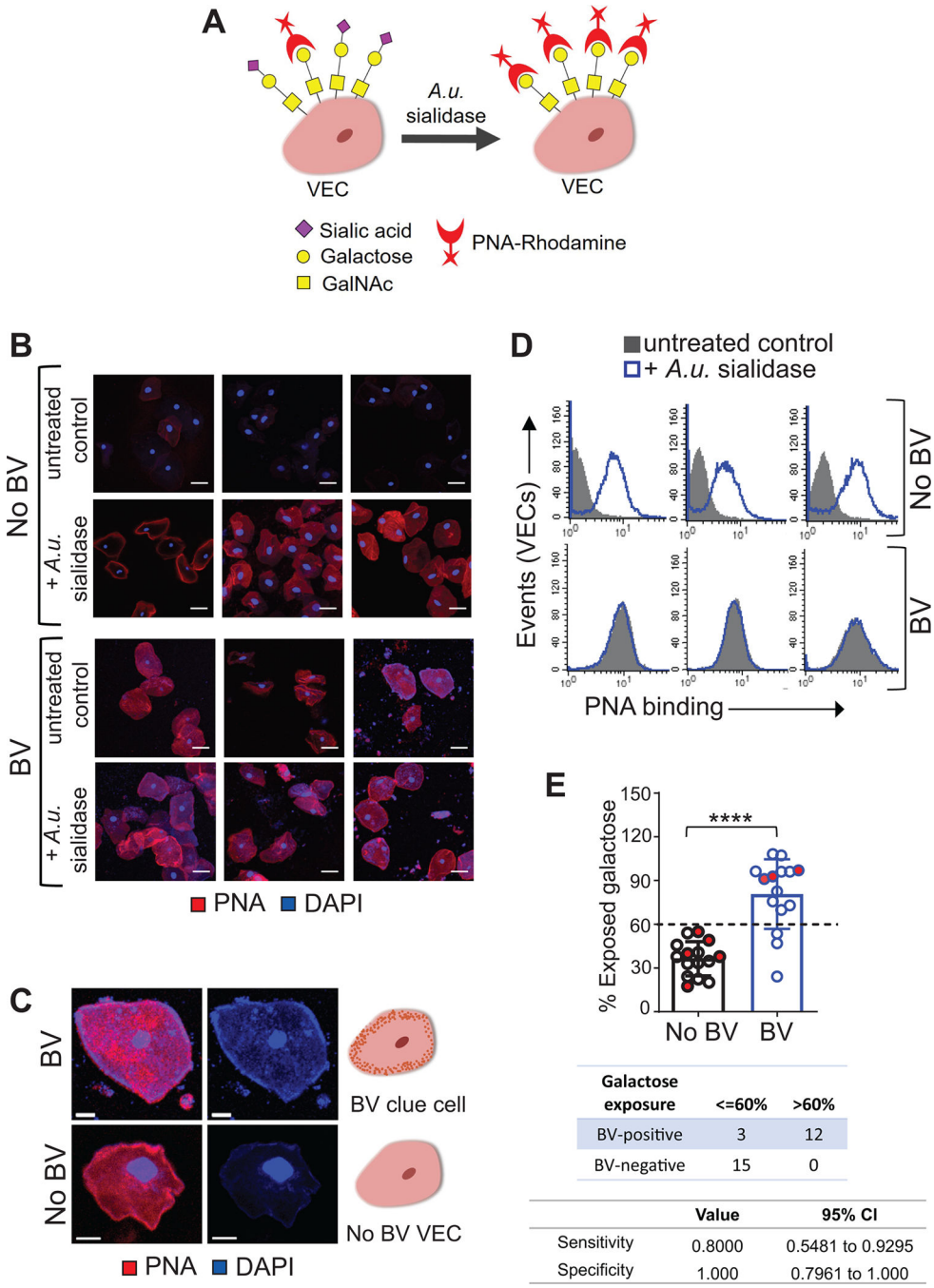

Galactose exposure	<=60%	>60%
BV-positive	3	12
BV-negative	15	0

	Value	95% CI
Sensitivity	0.8000	0.5481 to 0.9295
Specificity	1.000	0.7961 to 1.000

FIG. 4. Exposed galactose on the VEC surface in BV.

(**A**) Schematic: PNA-Rhodamine (PNA-Rh) binds to galactose residues, not masked by sialic acids, on VECs untreated or treated with sialidase. *A.u.* sialidase = sialidase from *Arthrobacter ureafaciens*. (**B**) Representative confocal images of PNA (red) stained VECs are shown from n=6 individual specimens. Images in the top and bottom are from the same specimen pretreated with exogenous sialidase (+*A.u.* sialidase) or with buffer alone (−*A.u.* sialidase, untreated control). Nuclei and bacterial cells (blue) are stained with DAPI. Images shown are representative of multiple fields of view for each specimen. Scale bars = 30 μm.

(**C**) Representative image of a BV epithelial cell with surface bacteria observed as blue puncta close to the cell membrane, indicative of clue cells. Scale bars = 10 μm. (**D-E**) Flow cytometry quantification of PNA binding to BV and No BV VECs pretreated with exogenous sialidase (*+A.u.* sialidase) or buffer alone (untreated control). (**D**) Representative histogram overlays are shown from n=6 individual specimens. (**E**) Estimation of percentage cell surface exposed galactose residues, calculated as percentage ratio of mean fluorescence intensity (MFI) of PNA binding to untreated VECs versus VECs pretreated with *A.u.* sialidase (n=15 samples per group). When possible, data points on the graph represent epithelial cells from individual women (n=22, black/blue circles). However, some data points represent pooled samples from 2–5 women (when recovery yielded insufficient cell quantity for flow cytometry) (N=8 pools, circles filled with red). Data in **B-E** is combined from 3 independent experiments. Error bars on the graph show standard deviation for each group. Statistical analysis by Mann–Whitney U, ****P<0.0001. Sensitivity and specificity values were determined using two-sided Fisher's exact test, with a galactose exposure threshold of 60% compared to the Nugent method. A total of n=46 specimens from individual women were used to generate the data in B-E. See methods for pooling rationale.

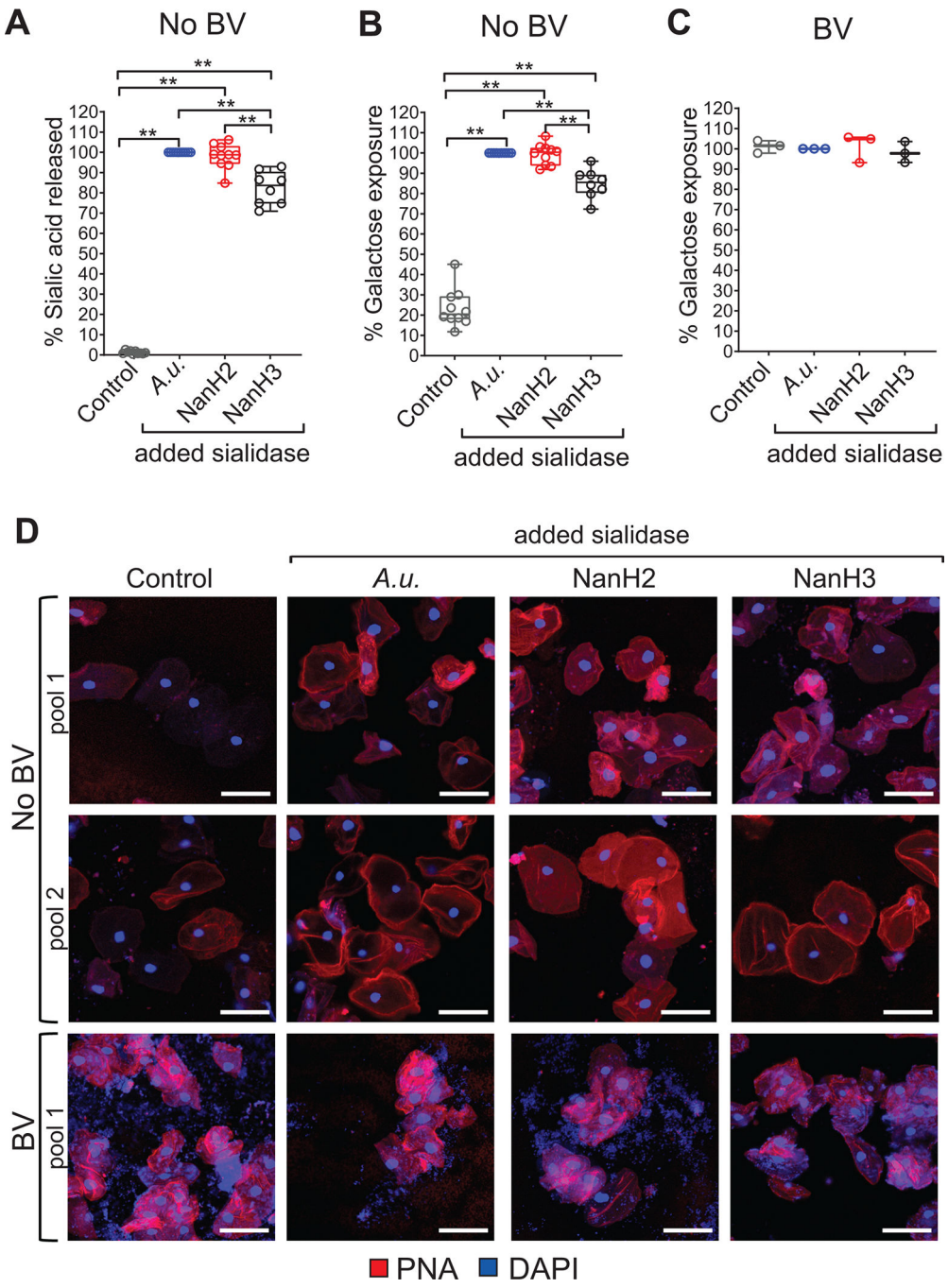

FIG. 5. Epithelial cells emulate BV phenotypes when treated with *Gardnerella* sialidases.

(**A-D**) Cells from the same pool of VECs, from women with or without BV, were treated with emply vector (Control), commercial *Arthrobacter ureafaciens* sialidase (*A.u.*), recombinant *Gardnerella* NanH2 sialidase (NanH2), or recombinant *Gardnerella* NanH3 sialidase (NanH3) as indicated. **(A)** Fluorimetric quantification of sialic acid (Neu5Ac) released from No BV VECs treated with either vector control or sialidase enzymes. (**B, C**) Flow cytometry analysis of PNA binding to VECs. Galactose exposure was assessed by comparing PNA binding to *A.u.* sialidase treated cells from the same pool. (**B**) Galactose

exposure on No BV VECs. (**C**) Galactose exposure on BV VECs (N=3 pools, with n=2–3 specimens in each pool). **(D)** Representative confocal images of VECs from women with and without BV, stained with PNA (red) lectin under control/sialidase treated condition. Nuclei and bacterial cells (blue) are stained with DAPI. Each row shows analysis of one pooled specimen. Scale bars are 50 μm. Data in **A-D** combined from 2 independent experiments. For No BV groups treated with vector control, *A.u.* sialidase, or *G.v.* NanH2 sialidase - N=10 pools, with n=2 – 5 specimens in each pool; for the No BV group treated with *G.v.* NanH3 sialidase- N=8 pools, with n=2 – 5 specimens in each pool. **p<0.01 (Wilcoxon signed rank test). A total of n=38 specimens from individual women were used to generate the data in **A-D**. Data in **6A**, **6B**, and **6D** are from the same No BV VEC pools. Data in **6C** and **6D** are from the same BV VEC pools. See methods for pooling rationale.

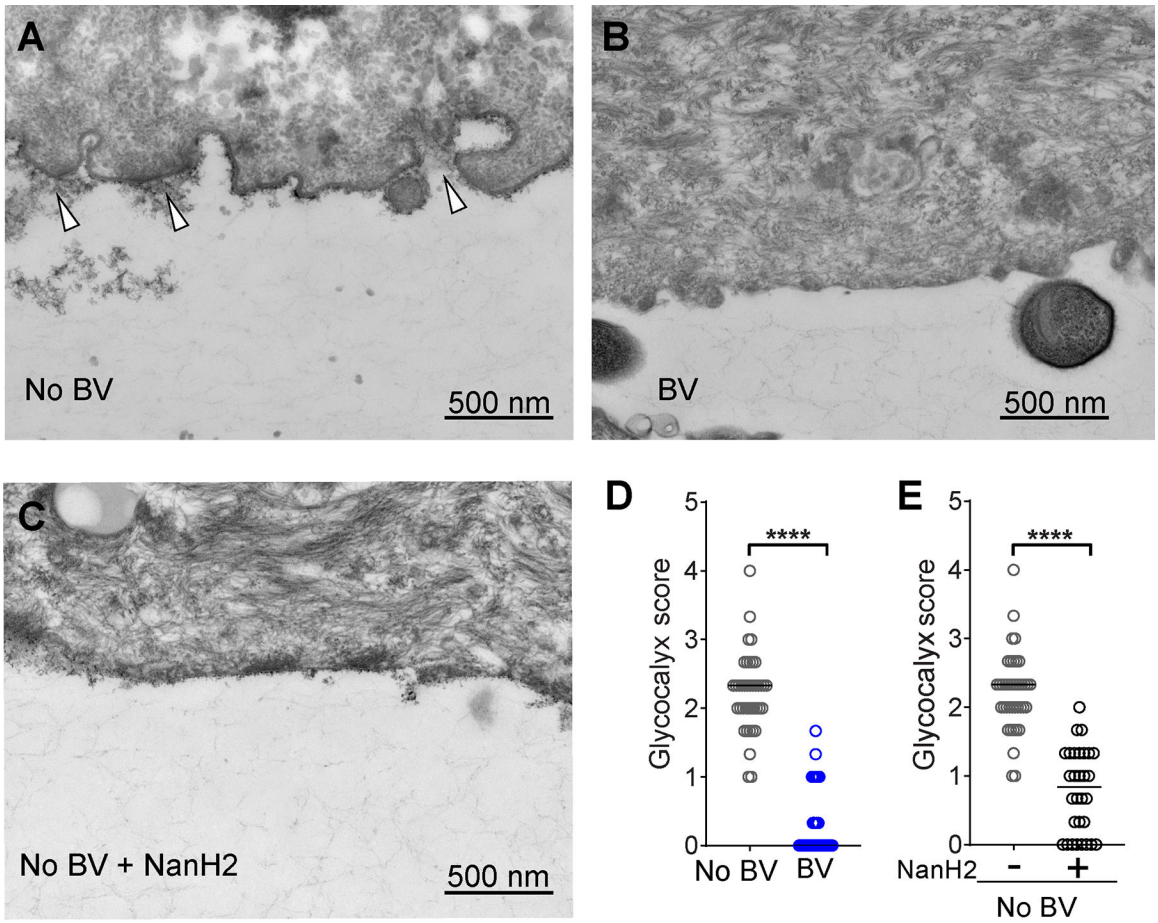

FIG. 6. The epithelial glycocalyx appears degraded in BV and *Gardnerella* sialidase is sufficient to establish this phenotype.

(A to C) Representative transmission electron microscopy (TEM) images of VECs from (**A**) No BV specimens - glycocalyx appears as a fuzzy layer close to epithelial cell membrane (indicated with arrowheads), (**B**) BV specimens, and (**C**) No BV specimens treated with recombinant *Gardnerella* sialidase (NanH2). (**D, E**) Pooled VECs from three of the No BV specimens were divided in half; one half was untreated (D) and the other half treated with recombinant *Gardnerella* NanH2 (E). Abundance of the glycocalyx was scored on a 0–4 scale, where four is “abundantly present” and zero is “none visible”. A total of ten TEM images were scored from each specimen (scoring rubric in fig. S11). Data points in the graph represent the average of three scores for each image. For No BV, N=40 images from n=4 specimens (same data in shown in **D** and **E**); BV, N=30 images from n=3 specimens; and No BV treated with NanH2, N=30 images from n=3 specimens. Images were acquired in a blinded fashion and scored by three observers blinded to the BV-status of the sample. All images were acquired at 25,000 X. Scale bars are 500 nm. ****$p<0.0001$ (Kruskal-Wallis with Dunn’s multiple comparisons test). A total of n=7 specimens were used to generate these data.

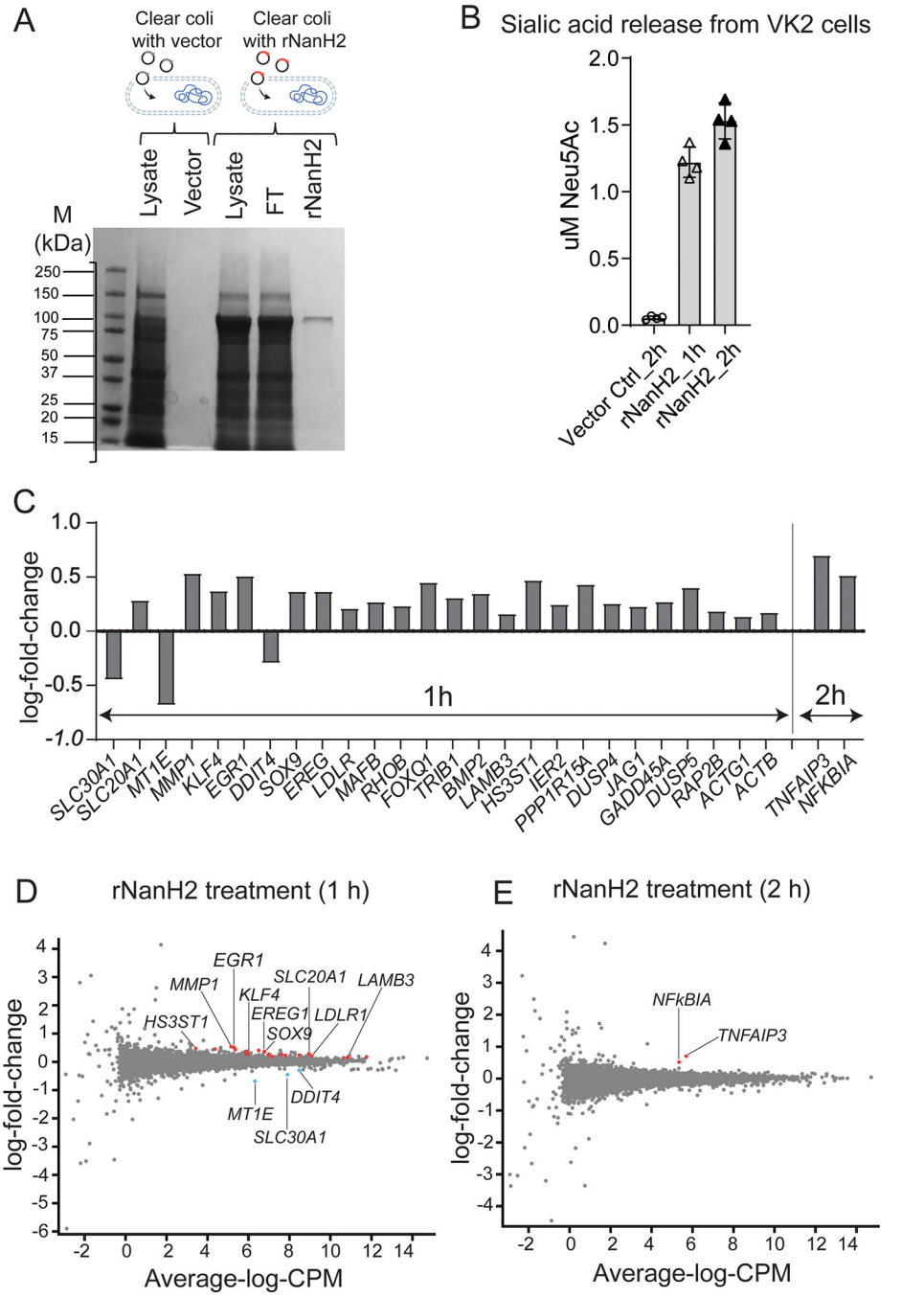

FIG. 7. Treatment with *Gardnerella* sialidase NanH2 alters transcriptomic profile of the vaginal epithelial (VK2) cells.

(**A**) SDS-PAGE analysis of recombinant NanH2 expression in ClearColi BL21(DE3). M: Molecular weight marker; rNanH2 (100 kDa). Schematic above the gel depict plasmids without or with truncated *nanH2* gene (red) used for transformation of ClearColi cells. (**B**) Fluorimetric quantification of DMB-labelled sialic acid (Neu5Ac) from VK2 cells treated with vector or rNanH2. (**C**) Fold-change for all the genes that were significantly altered (adj. p value < 0.05), at both 1 h and 2h, is shown in the bar graph. (**D-E**). Genes

that had altered expression in VK2 cells treated with rNanH2, as compared to the vector control, are indicated in the scatterplots with expression (log cells per million [CPM]) shown on the x-axis and log-fold-change shown on the y-axis. Here, red dots denote genes that were significantly up-regulated and blue dots denote genes that were significantly down-regulated, with adj. p value < 0.05. Schematics were created with BioRender.com.

Table 1.

Gene set enrichment analysis identifies pathways enriched in VK2 cells treated with *Gardnerella* sialidase rNanH2

Pathways enriched in VK2 cells after 1-h rNanH2 treatment			
Gene ontoloav bioloaical process term	NES *	P value	Adj. P value
BIOLOGICAL_ADHESION	2.30	8.32–0e	1e–28
CELL_MIGRATION	2.23	3.4e–31	1.0e–27
LOCOMOTION	2.15	4.0e–31	1.0e–27
TISSUE_DEVELOPMENT	2.07	4.1e–29	7.8e–26
RESPONSE_TO_OXYGEN_CONTAINING_COMPOUND	2.11	4.9e–27	7.4e–24
REGULA TION_OF_CELLULAR_ COMPONENT_MO VEMENT	2.23	4.9e–24	6.2e–21
STRUCTURE FORMATION INVOLVED IN MORPHOGENES IS	2.19	1.0e–23	1.1e–20
REGULA TION_OF_CELL_ POPULA TION_PROLIFERA TION	1.99	1.1e–21	1.1 e–18
RESPONSE_TO_OXYGEN_CONTAINING_COMPOUND	2.12	1.4e–21	1.2e–18
VASCULA TURE_DE VELOPMENT	2.26	4.5e–20	3.4e–17
GOBP_PROTEIN_FOLDING	−1.75	3.5e–05	8.4e–04
Pathways enriched in VK2 cells after 2-h rNanH2 treatment			
Gene ontology biological process term	NES *	P value	Adj. P value
PROGRAMMED_CELL_DEA TH	1.68	1.5e-14	1.1e-10
INTERSPECIES_INTERACTION_BETWEEN_ORGANISMS	1.76	1.2e-13	4.4e-10
REGULA TION_OF_CELL_DEA TH	1.69	6.2e-13	1.6e-09
REGULATION_OF_IMMUNE_SYSTEM_PROCESS	1.74	4.7e-11	9.0e-08
RESPONSE_TO_MOLECULE_OF_BACTERIAL_ ORIGIN	2.35	1.0e-10	1.6e-07
CELLULAR_RESPONSE_TO_BIOTIC_STIMULUS	2.23	4.0e-10	5.1e-07
TOLL_LIKE_RECEPTOR_SIGNALING_PATHWAY	2.37	9.3e-10	1.0e-06
IMMUNE_RESPONSE	1.63	1.2e-09	1.1e-06
RESPONSE_TO_MOLECULE_OF_BACTERIAL_ ORIGIN	2.08	2.3e-09	2.0e-06
POSITIVE REGULATION OF PROTEIN METABOLIC PROC ESS	1.55	5.5e–09	3.9e–06

* NES : Normalized Enrichment Score based on fGSEA analysis